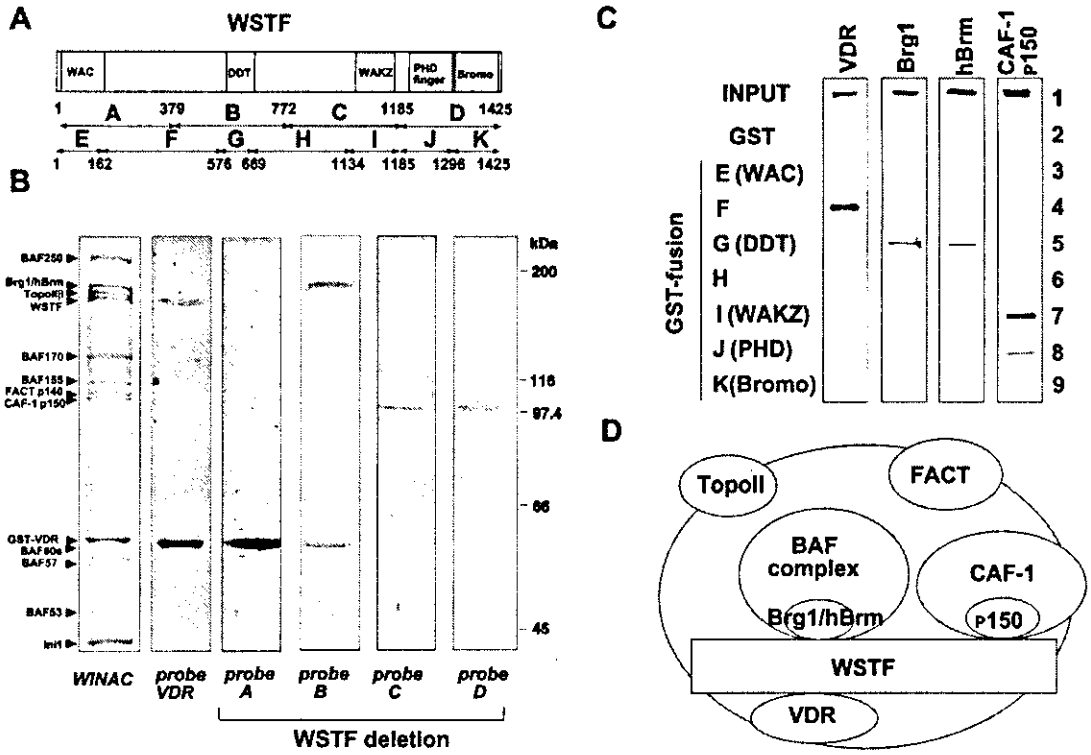

Figure 3. WSTF as a Platform Protein in WINAC

(A) Schematic representation of the probes used for the Far Western blotting and the GST pull-down assay. WSTF deletion mutants are expressed as GST-chimeric proteins.

(B) Far Western blotting of the WINAC complex probed with indicated ^{32}P-labeled GST-fused chimeric proteins. ^{32}P-labeled GST-fused chimeric proteins were prepared with pGEX-2TK vector (Amersham Biosciences) by PKA phosphorylation (Rachez et al., 1998).

(C) Physical interaction of WINAC components and VDR with WSTF deletion mutants in GST pull-down assay.

(D) Schematic representation of the interacting domains of WSTF.

SNF-type complexes, PBAF, which was purified and identified by in vitro transcription to coactivate VDR in a ligand-dependent manner (Lemon et al., 2001). Interestingly, WINAC appears to harbor three components (TopoIIβ, FACTp140, and CAF-1p150) (Smith and Stillman, 1989; Varga-Weisz et al., 1997; LeRoy et al., 1998), which have not yet been found in any known ATP-dependent chromatin-remodeling complexes. Western blotting with specific antibodies verified several WINAC components (Figure 2D). Moreover, major WINAC components in a purified endogenous complex associating with VDR were detected (Figure 2E), supporting presence of WINAC as a stable complex in native cells.

Clear retention of VDR was detected upon the WSTF band, but not the other subunits (Figure 3B), confirming the GST-pull-down assay results (Figure 1D). The WSTF fragments were trapped on not only VDR but also CAF-1p150 and Brg1/hBrm (Figure 3B). Such interactions were also seen in the expected regions by the GST-pull-down assay (Figure 3C), suggesting that WSTF serves as a platform subunit to assemble components into WINAC (as illustrated in Figure 3D).

WINAC Is a Multifunctional ATP-Dependent Chromatin-Remodeling Complex

We then examined if purified WINAC exerts an ATP-dependent chromatin-remodeling activity by comparing its activity with a complex of the recombinant dAcf1 and dISWI proteins in a standard micrococcal nuclease assay. This recombinant complex has been reported sufficient to mobilize nucleosomes in vitro in an ATP-dependent manner (Ito et al., 1997). Like the dISWI complex, an ATP-dependent chromatin-assembly reaction was clearly induced by WINAC (compare lanes 6, 7, and lane 3 in Figure 4A), indicating that Brg1/hBrm in WINAC serves as an ATPase for this ATP-dependent chromatin-remodeling process. WINAC appeared to have a chromatin-assembly activity (data not shown) like RSF (Loyola et al., 2001).

We then examined the ability of WINAC to disrupt nucleosome arrays through VDR bound DNA since the known ATP-dependent chromatin-remodeling complexes are potent to recognize the nucleosomal array around the binding sites of a sequence-specific regulator (Ito et al., 1997; Lemon et al., 2001). By Southern blot analysis with a pair of oligonucleotides complementary to a region in the vicinity (promoter probe) or to a site about 900 bp upstream (distal probe) of the GAL4 DBD binding sites for a chimeric VDR-DEF protein (GAL-VDR), disruption of the nucleosome arrays in the GAL4 binding site vicinity was induced only when both VDR and WINAC were present (lane 4 in Figure 4B), while the other regions appeared unaffected in the nucleosome arrays (Figure 4B). Reflecting the VDR-specific nucleo-

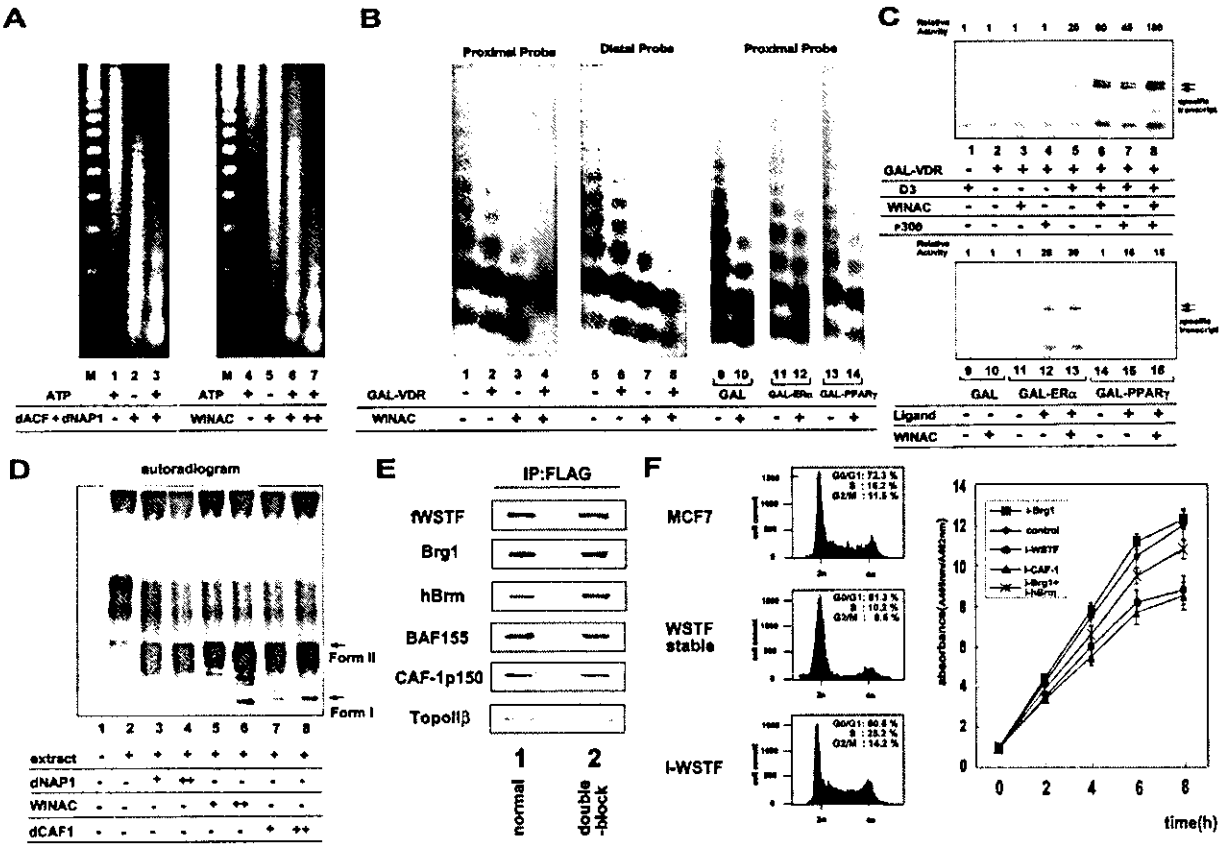

Figure 4. WINAC as an ATP-Dependent Chromatin-Remodeling Complex

(A) Chromatin-reconstitution activity of WINAC. The reacted samples were subjected to partial micrococcal nuclease digestion. The molecular mass marker (M) is the 200 bp ladder.

(B) Chromatin disruption by WINAC is specifically VDR dependent. Oligonucleotide probe corresponds to either a sequence between the GAL4 sites and the RNA start site (proximal probe) or 900 bp upstream of the start site (distal probe).

(C) Potentiation of VDR transactivation by WINAC in vitro. Arrows indicate specific transcripts by transcription reactions by GAL4 derivatives. A representative result is displayed, and relative activities were calculated from three independent assays with pGl0 vector as an internal control.

(D) WINAC functions as a chromatin-reconstitution factor during DNA replication in vitro. During DNA replication induced by SV40 T antigen in vitro, WINAC could form chromatin with negatively supercoiled DNA. Form I, a perfect supercoiled DNA; form II, a relaxed form.

(E) WINAC formation is unchanged in S phase. MCF7 stable transformants were cultured under either normal conditions or double-thymidine block treatments.

(F) Modulation of the cell cycle by altered WSTF expression. Left image: DNA histogram of the MCF7 cells [MCF7], WSTF stably expressing MCF7 cells [WSTF stable] and MCF7 cells transfected with WSTF-RNAi [I-WSTF]. Right image: BrdU incorporation during S phase of the MCF7 cells transfected with RNAi from the indicated proteins during double-thymidine treatment. After the final release (time 0), cells were collected every 2 hr, for up to 8 hr. The average values of triplicate analyses are shown.

some disruption by WINAC among tested receptors (Figure 4B), ligand-induced transactivation in vitro was potentiated by WINAC for VDR, but for neither ERα nor PPARγ (Figure 4C).

WINAC Function during DNA Replication

The WINAC function in DNA replication (Smith and Stillman, 1989; Varga-Weisz et al., 1997) was addressed by reconstituting chromatin structure upon newly replicated DNA by an in vitro assay. WINAC, like the reported CAF-1 histone chaperone complex (see lanes 7 and 8 in Figure 4D), could facilitate forming chromatin structure with negatively supercoiled DNA on newly replicated DNA through nucleosome arrangement (Smith and Stillman, 1989) (Figure 4D). Moreover, WINAC complex formation was detected irrespective of the cell-cycle stages, even when blocked at S stage by double-thymidine treatments (Fujita et al., 1996) (Figure 4E). Manipulation of WSTF expression by WSTF-RNAi expression (Elbashir et al., 2001) resulted in alterations in the cell cycle (left images in Figure 4F). Particularly, DNA synthesis was clearly lowered by RNAi expression of either WSTF or Brg1/hBrm ATPases (right image in Figure 4F). Thus, these findings suggest that WINAC plays a role in chromatin remodeling during DNA replication.

WSTF Coactivated Ligand-Induced Transactivation Function of VDR

Next, we investigated if WSTF potentiates the ligand-induced transactivation of VDR in MCF7 cells by transient expression analysis. 1α,25(OH)2D3 (10^{-9} M) was effective to induce VDR AF-2 transactivation function.

WSTF coactivated this ligand-induced AF-2 function of VDR, but not ERα (compare lanes 3 and 4 with 23 and 24 in Figure 5A). Both Brg1 and hBrm were potent to enhance the transactivation functions of VDR and ERα (compare lanes 9 and 12 with lane 2 for VDR; lanes 29 and 32 with lane 22 for ERα in Figure 5A) as previously reported (Chiba et al., 1994; DiRenzo et al., 2000; Shang et al., 2000; Belandia et al., 2002). Interestingly, such coactivator-like activity of WSTF was selective for VDR, and not detected for ERα, even in the presence of Brg1/hBrm (see lanes 30 and 33 in Figure 5A).

To confirm such a coactivator-like function of WSTF for VDR, the ligand-induced transactivation function of VDR was assessed 40 hr after the RNAi transfection and was severely attenuated nearly to basal transcription levels (lanes 7 and 8 in Figure 5A). Interestingly, WSTF-RNAi expression was found to also abrogate the VDR coactivation of the VDR transcriptional activity by the known NR coactivators, such as TRAP220 and TIF2 (lanes 16 and 18 in Figure 5A). Similarly, RNAi expression resulted in a loss of the coactivator-like function of WSTF for VDR when intact VDR/RXR heterodimer was bound to a naturally occurring positive vitamin D response element (VDRE) derived from the human 1α,25-dihydroxyvitamin D3 24-hydroxylase [24(OH)ase] gene promoter (Chen and DeLuca, 1995) (Figure 5C). ChIP analysis revealed that VDR and the WINAC components were constitutively associated with the promoter irrespective of ligand binding. In the contrast, ligand-induced occupancy in the promoter was seen in TRAP220 and TIF2 with ligand-induced histone H4 acetylation (compare lane 3 with 4 in Figure 5B), though the ligand-induced TRAP220 and TIF2 occupancy was cyclic (data not shown) as expected from previous reports (Shang et al., 2000). Such ligand-dependent and -independent recruitments of factors to the promoter were robustly attenuated by WSTF-RNAi expression (lane 5 in Figure 5B).

As the VDR/RXR heterodimer also represses transcription in a ligand-dependent manner through negative VDRE (nVDRE), the action of WSTF in the ligand-induced transrepression was examined in a naturally occurring nVDRE in human 25-hydroxyvitamin D3 1α-hydroxylase [1α(OH)ase] (Murayama et al., 1998). ChIP analysis uncovered that VDR and WINAC appear to land on the nVDRE in a ligand-independent manner, while ligand-induced (compare lane 8 with 9 in Figure 5B), but cyclic (data not shown) recruitments of N-CoR and HDAC2 were observed. Ligand-dependent repression was exaggerated by WSTF overexpression (lanes 3 and 4 in Figure 5D), but attenuated again by WSTF-RNAi expression (lanes 5 and 6 in Figure 5D). Thus, it is likely that WINAC association with VDR facilitates targeting of a putative corepressor complex to the nVDRE. The WINAC function in the native VDR target gene promoters and the endogenous gene expressions of 24(OH)ase and 1α(OH)ase were further confirmed by the impaired 1α,25(OH)2D3 responsiveness by the WSTF ablation (Figure 5E). Thus, these findings point out that WINAC rearranges the nucleosome array around the positive and negative VDREs, thereby facilitating the coregulatory complexes accessible to VDR for further transcription control.

Impaired Transactivation Function of VDR Was Recovered by WSTF Overexpression in Williams Syndrome Patients

Together with these observations, the typical phenotypes of the WSTF gene-deleted WS patients (Taylor et al., 1982; Garabedian et al., 1985) prompted us to assume that a lowered WINAC function caused by reduced WSTF expression may result in aberrant chromatin remodeling, leading to diverse abnormalities, including abnormal vitamin D metabolism and hypercalcemia. Considering WSTF and VDR skin expression (Yoshizawa et al., 1997), we first assessed the ligand-induced transactivation function of VDR in skin fibroblast cells derived from three normal and three WS patients, in which the region covering the WSTF gene is deleted in one chromosome 7 allele, as representatively shown in patient #1 by FISH analysis (Figure 6A). Northern blot analysis unmasked the WSTF expression levels were clearly lowered (~50%) in the WS patients (Figure 6B). By a transient transfection assay in fibroblast cells, we found reduced transactivation function of VDR in the WS patient cells (Figure 6C). Consistent with the impaired function of VDR in the WS cells, the ChIP analysis showed robust reduction in targeting of VDR, the WINAC components, and the coactivators to the 24(OH)ase VDRE (lanes 9 and 10 in Figure 6E), in agreement with the MCF7 cell results (Figure 5B).

Most strikingly, WSTF expression by an adenovirus vector (Kitagawa et al., 2002) could rescue the reduced responsiveness of 24(OH)ase gene induction by 1α,25(OH)2D3 for 12 hr in the WS skin fibroblasts (compare lane 3 with 4 in Figure 6D), with the impaired promoter targeting of the WINAC components and unliganded recoveries in VDR to the 24(OH)ase promoter (see lane 11 in Figure 6E), and the impaired ligand-induced recruitment of the NR coactivators (see lane 12 in Figure 6). Thus, these findings suggest that at least a part of the endocrine disorders found in the WS patients are related to VDR malfunction caused by the lowered WINAC function, which is due to lower WSTF expression.

The WSTF transcript during embryogenesis was not detected by Northern blotting, but detectable by RT-PCR (Figure 7A). By whole mount in situ staining (Sekine et al., 1999) at 9.5 dpc, the WSTF transcript appeared to be ubiquitously expressed (data not shown), but its expression pattern became limited and partially overlapped with mouse Brg1 and BAF155 (Srg3) expression (Bultman et al., 2000; Kim et al., 2001) as evident at 11.5 dpc (Figure 7B). Surprisingly these expression patterns seem different from that of mouse Snf2h (Lazzaro and Picketts, 2001), particularly at brain. These results may suggest a specific role of WINAC during embryogenesis, which may account for the diverse abnormalities in the WS patients.

Discussion

Purification and Identification of a Human Multiprotein Complex Containing WSTF, WINAC

WINAC contains known components of the hSWI/SNF-type complexes, including two major ATPase subunits, Brg1 and hBrm (Figure 2C). However, by our purification

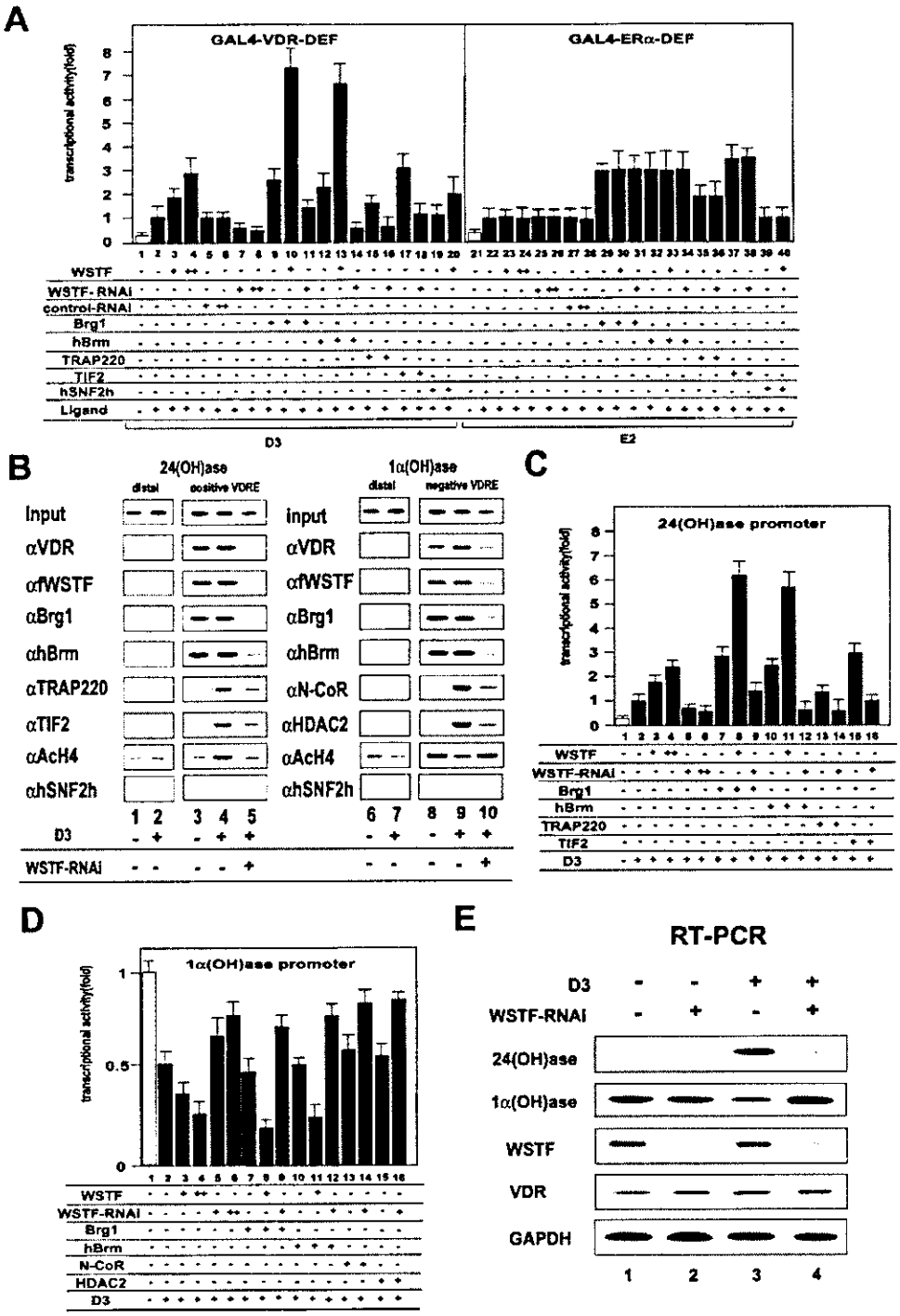

Figure 5. Ligand-Dependent Promoter Targeting of Coregulators through WINAC-VDR Association

(A) VDR-specific facilitation of co-activator accessibility by WINAC. MCF7 cells were transfected with the expression vectors of a luciferase reporter plasmid containing the GAL4 upstream activation sequence (UAS) [17mer(×2)] driven by the β-globin promoter (0.5 μg). PML-CMV (2 ng); GAL4-DBD-VDR-DEF (0.2 μg); GAL4-DBD-ERα DEF (0.2 μg); pDNA3-FLAG-WSTF (+; 0.1 μg: ++; 0.3 μg); pSV-Brg1 (0.2 μg); pSV-hBrm (0.2 μg); pcDNA3-TRAP220 (0.3 μg); pcDNA3-TIF2 (0.3 μg); siRNA (+; 0.1 μg: ++; 0.2 μg) of WSTF-RNAi; or control RNAi or their combinations were transfected as indicated in the images in the absence or presence of ligand (10^{-9} M). Bars in each graph show the fold change in luciferase activity relative to the activity of the receptor transactivation in the presence of ligand.

(B) ChIP analysis on the 24(OH)ase promoter and 1α(OH)ase promoter of WSTF stable transformants. Soluble chromatin was prepared from WSTF stable transformants treated with D3 (10^{-9} M) for 45 min and immunoprecipitated with indicated antibodies.

(C and D) The coregulator-like actions of WSTF on the naturally occurring positive and negative vitamin D response elements. MCF7 cells were transfected with the expression vectors of either the luciferase reporter plasmid containing a human 24(OH)ase promoter harboring a canonical positive VDRE or a human 1α(OH)ase promoter containing a negative VDRE and the factors shown in (A) or together with pcDNA3-N-CoR (0.3 μg), pcDNA3-HDAC2 (0.3 μg).

(E) WSTF-mediated regulations of endogenous genes by VDR. RT-PCR analysis of MCF7 cells was performed 12 hr after the induction by D3 (10^{-9} M) (Yanagisawa et al., 2002).

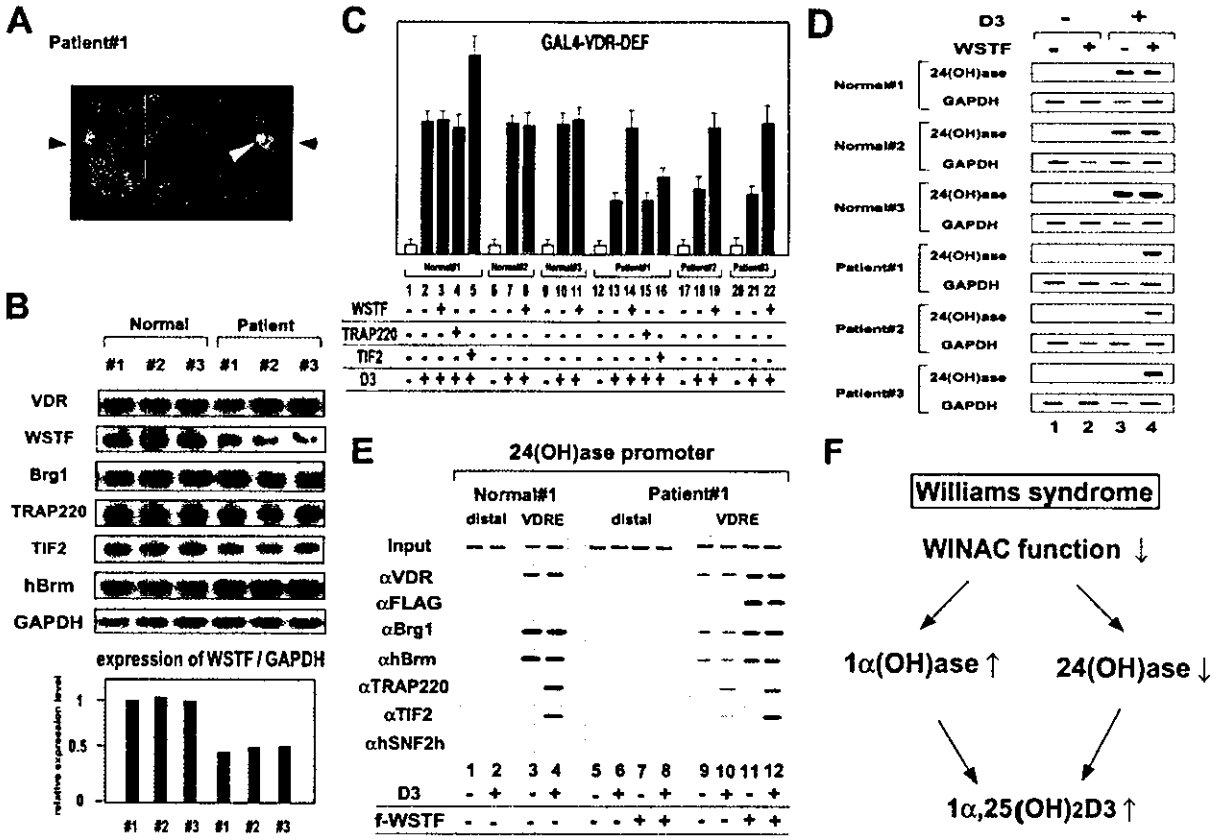

Figure 6. Impaired VDR Function in the Fibroblasts of Williams Syndrome Patients Was Recovered by WSTF Overexpression

(A) Fluorescence in situ hybridization of WS patient 1, confirming a deletion of one copy of the WSTF gene. The black arrowhead indicates D7S427 gene locus and the white arrowhead for WSTF gene. D7S427 was used for a chromosome 7 marker and cosmid full-length WSTF for WSTF gene probe.

(B) Reduced WSTF expression levels in WS skin fibroblasts. The indicated genes were examined for expression by Northern blotting with GAPDH expression as an internal control (Yanagisawa et al., 2002). Densitometric analysis of the relative expression level of WSTF versus GAPDH is shown in the lower image.

(C) VDR transactivation functions were impaired in the skin fibroblasts of the WS patients. Fibroblasts from controls and patients were transfected with the expression vectors as described in Figure 5A and the receptor function was tested.

(D) WSTF overexpression recovered the impaired responsiveness to vitamin D during 24(OH)ase gene induction. Patient's skin fibroblasts were transfected with an adenovirus expressing FLAG-WSTF, and treated with 1α,25(OH)2D3 (10^{-9} M) for 12 hr. Total RNA was subjected to RT-PCR analysis of 24(OH)ase expression.

(E) Impaired promoter targeting of VDR, coregulators, and WINAC components in fibroblasts from WS patients was rescued by WSTF overexpression. ChIP assays of the patient skin fibroblasts were performed with adenovirus expressing FLAG-WSTF as described in Figure 5B.

(F) Hypothesis of the cause of hypercalcemia in Williams syndrome patients.

methods we could detect neither the PBAF complex nor its specific component (BAF180). Moreover, by our purification, no ISWI-based complex was detectable even in the glycerol gradient fractions containing complexes with expected molecular weights. These observations are also different from a report that WSTF forms a hISWI-based chromatin-remodeling complex (Bozhenok et al., 2002). Confirming that hISWI (hSNF2h) expression did not affect the VDR transactivation function (Figures 5A and 5B), the combination with ISWI-based complex components looks to deter WSTF from the VDR interaction.

Of note, WINAC harbors three components, which have not yet been found in the ATP-dependent chromatin-remodeling complexes. Two factors (CAF-1p150 and TopoIIβ are integrated in the complexes serving roles in DNA replication (Smith and Stillman, 1989; Varga-Weisz et al., 1997), while FACT p140 is involved in a complex that promotes chromatin-dependent transcriptional elongation with an ISWI-type complex (LeRoy et al., 1998). From the observed WSTF interactions with the other subunits in vitro (Figures 3A–3D), WSTF appears to serve as a core protein to form an SWI2/SNF2-based complex, generating a subclass of the ATP-dependent chromatin-remodeling complex with DNA replication-related factors. Taken together, WSTF may serve as a dual platform protein capable of forming both SWI/SNF- and ISWI-type chromatin-remodeling complexes by distinct subunit combinations, but only the SWI/SNF-type WINAC selectively assists VDR function through a physical interaction.

WINAC Is a Chromatin-Remodeling Complex

Specific and more efficient targeting of VDR through WINAC to the VDREs was supported from functional analyses of the purified WINAC in vitro. In this respect,

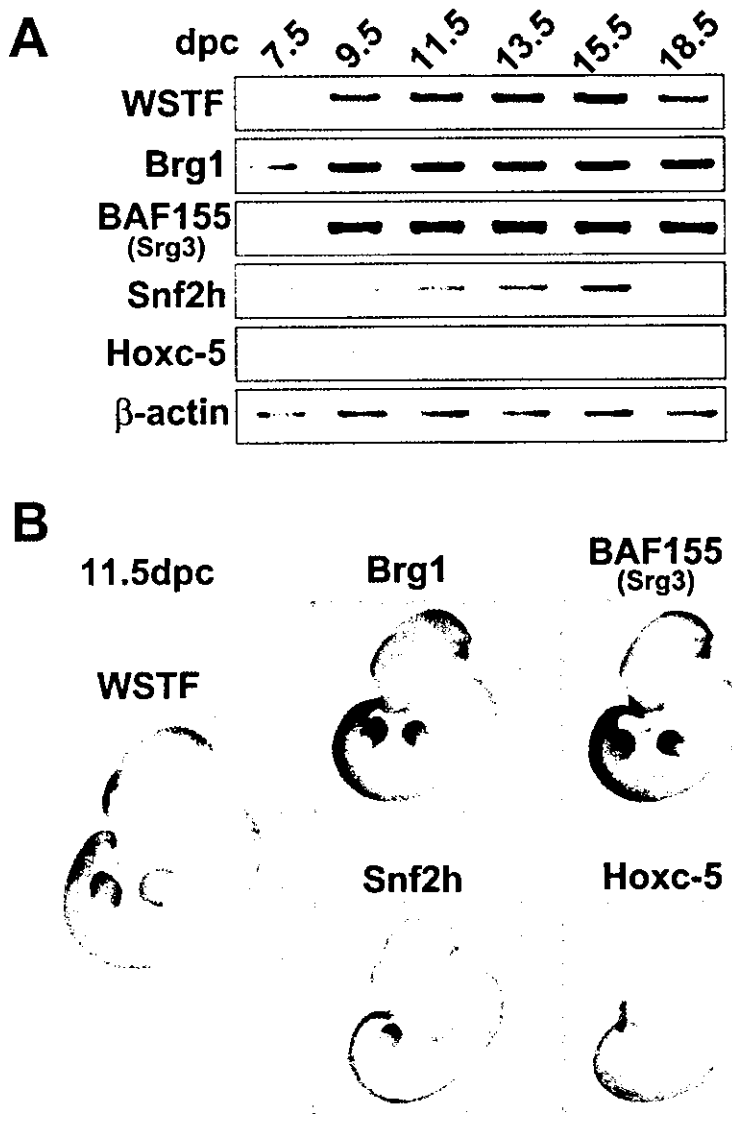

Figure 7. Spatiotemporal Expression Patterns of WSTF during Mouse Embryogenesis

(A) RT-PCR analysis of mouse WSTF, Brg1, BAF155 (Srg3), Snf2h, Hoxc-5, and β-actin gene expression. Embryos were dissected at the indicated times (7.5 dpc to 18.5 dpc). Samples were normalized by dilution to give equivalent signals for β-actin.

(B) Whole mount in situ hybridization analysis of mouse WSTF, Brg1, BAF155 (Srg3), Snf2h, and Hoxc-5 (negative control) expression at 11.5 dpc (Scale bar: 2 mm. Sense control probes were also hybridized and no signal was detected; data not shown).

WINAC subunit configuration is of interest to be clarified for defining the function of each component. A recent report has revealed that the chromatin-remodeling activity of the dISWI-based complex requires multiple Acf1 motifs to nonspecifically anchor DNA through its WAC motifs, and to directly interact with ISWI through the DDT domain (Fyodorov and Kadonaga, 2002). In addition to a core subunit role of WSTF, multiple functions as a pivotal factor to conduct the WINAC function could be further speculated from the conservation of several motifs that are shared with the other WAC family proteins, like hACF1 (Jones et al., 2000). Moreover, functions of the bromodomain and PHD finger motif in WSTF remain to be established in the promoter targeting and chromatin remodeling (Hassan et al., 2002; Schultz et al., 2002).

Promoter Targeting of VDR by WINAC and Cooperative WINAC Function with the Coregulator Complexes

Similar to the reported coactivator-like actions of the SWI2/SNF2 ATPases and BAF57 for the ligand-induced ERα transactivation (Chiba et al., 1994; DiRenzo et al., 2000; Belandia et al., 2002), overexpression of WSTF and the ATPase subunits as well could coactivate the ligand-induced VDR transactivation as either a GAL4 DBD chimeric protein or heterodimer with RXR (Figures 5A and 5C). VDR coactivation by the ligand-dependent NR coactivators (TIF2 and TRAP220) was abrogated by WSTF-RNAi expression (Figure 5A). However, neither such coactivator-like WSTF actions nor reduced coactivation by NR coactivators by the WSTF-RNAi expression was detected for ERα (Figure 5A) and the other receptors tested (data not shown), supporting the observed direct and selective interaction of WSTF with VDR among NRs (Figure 1D). Moreover, WSTF overexpression potentiated the ligand-induced transrepression of VDR on the 1α(OH)ase negative VDRE (Figure 5D), where an ablation of endogenous WSTF by RNAi expression led to a significant reduction in ligand-induced corepressor recruitment (lane 10 in Figure 5B). Thus, ligand-independent association of WINAC and VDR in the VDR target promoters appears to facilitate the local nucleosomal array

accessibility for ligand-dependent coregulators, following histone tail modifications by the recruited coregulator complexes (Hassan et al., 2002). It was recently reported that only when ligand is bound to ERα, all of the ERα p160/CBP HAT coactivator complex and human SWI/SNF-type complexes are targeted to the ER target promoters, although such ligand-induced occupancy of ERα and coregulator in the promoters appears in a cyclic fashion (Shang et al., 2000; Belandia et al., 2002). Such ligand-induced assembly of the SWI/SNF-type complexes with NRs through the p160/CBP complex might be a common mechanism for ligand-dependent targeting of NRs to the cognate promoters (Glass and Rosenfeld, 2000).

Unlike NRs such as ERα and AR (Belandia et al., 2002; Shang et al., 2002), VDR appears from ChIP analysis (Figure 5B) to be selectively targeted through WINAC to the promoters without ligand-induced activation of VDR function or following recruitment of coregulator complexes. WINAC targeting to the promoters appears not to require specific histone tail modifications by coregulators. Thus, it is likely that WINAC associating on promoters escort VDR for its recognition and specific binding to VDREs, through nucleosomal mobilization by WINAC, presumably cooperating with the other chromatin complexes (Lemon et al., 2001). Alternatively, once VDR happens to bind VDREs during nonspecific chromatin remodeling, WINAC might be acquired to VDR upon the promoters to engage in local nucleosome reorganization. The latter possibility coincides well with a recent report about a sequence-specific regulator, SATB1 (Yasui et al., 2002). As a result, the local chromatin structure near VDREs may transit into an active chromosomal state that appears competent for receipt of both the coactivator complexes and the corepressor complexes (Figures 5C and 5D) dependent on the VDRE sequences and the tertiary positions of DNA-bound VDR. This is not consistent with recent observations that the chromatin-remodeling complexes are recruited only after acetylation/deacetylation of histone tails by the coregulatory complexes (Hassan et al., 2002). However, the orders of the complex targetings are supposed to be dependent on the regulator type and the promoter context (Lomvardas and Thanos, 2002; Soutoglou and Talianidis, 2002).

Williams Syndrome Is a Chromatin-Remodeling Factor Disease?

We found that the ligand-induced transactivation function of VDR is impaired in the skin fibroblast cells of all three tested patients, in whom the regions covering the WSTF gene locus at the chromosome 7q11.23 are heterozygously deleted. Such impaired VDR function should not lead to severe defects in vitamin D actions in adults, since the adult VDR heterozygote mice ($VDR^{+/-}$) and the heterozygous carrier patients of the hereditary vitamin D-dependent type II rickets caused by VDR inactivation exhibited no overt abnormality in calcium and vitamin D metabolism, though VDR is a major regulator in those metabolisms (Yoshizawa et al., 1997). However, during growth, the mineral intakes must be greater than their excretions through the actions of calciotropic hormones, including vitamin D. It is tempting to speculate that the significantly reduced WINAC levels in WS patients transiently cause impaired function in VDR and other unidentified factors, leading to the transient appearance of infantile aberrant vitamin D metabolism and consequently, hypercalcemia (Taylor et al., 1982; Garabedian et al., 1985). These findings together suggest that a normal WSTF dose in the cells is necessary to support normal activities of VDR and presumably of some other regulators.

WSTF expression patterns during mouse embryogenesis overlap with those of the common components of WINAC (Bultman et al., 2000; Kim et al., 2001), but appear more limited. In contrast, the more restricted expression pattern was detected in mouse ISWI (Snf2h) (Lazzaro and Picketts, 2001) (Figure 7B). It is therefore possible to suggest that specific roles of WINAC among the other chromatin-remodeling complexes exert in a more spatiotemporal manner and support organogenesis of several selected tissues during embryogenesis through chromatin remodeling for, at least, transcription and DNA replication. Therefore, the WS patients may suffer a wide spectrum of disorders in certain organs. Thus, this study suggests that the Williams syndrome disorders are caused, at least in part, by WINAC dysfunction as a chromatin-remodeling disease.

Experimental Procedures

Plasmids and Antibodies

Chimeric GST proteins of GAL4 DBD (1–147 aa) fused with Rat VDR-DEF and WSTF deletion mutants were expressed in pGEX-2TK (Pharmacia Biotech). The promoter region of 1α,25-dihydroxyvitamin D3 24-hydroxylase (−367 to 0) and 25-hydroxyvitamin D3 1α-hydroxylase (−889 to−30) were inserted into the pGL3 vector (Promega) driven by a thymidine kinase (tk) promoter (Chen and DeLuca, 1995; Murayama et al., 1998; Yanagisawa et al., 2002). Rabbit polyclonal antipeptide antiserum was prepared by Sawady technology against KLQSEDSAKTEEVDEEKK, which is near the human WSTF C terminus.

Purification and Separation of VDR-Associated Complexes

For WINAC purification, the nuclear extracts of the MCF7 stable transformant were prepared by the same method as HeLa nuclear extracts (Rachez et al., 1998; Kitagawa et al., 2002; Yanagisawa et al., 2002). Then, they were bound to the GST column [GST], and 1α,25(OH)2D3-unbound GST-VDR column [GST-VDR(D3-)]. The complexes bound to the ligand-unbound VDR were eluted with 15 mM reduced glutathione in elution buffer (50 mM Tris-HCl [pH 8.3], 150 mM KCl, 0.5 mM EDTA, 0.5 mM PMSF, 5 mM NaF, 0.08% NP-40, 0.5 mg/ml BSA, and 10% glycerol). Next, they were layered on top of a 4.5 ml linear 100%–40% glycerol gradient in the GST binding buffer and centrifuged for 16 hr at 4°C at 40,000 rpm in a SW40 rotor (Beckman). Protein standards were ovalbumin (44 kDa), β-globulin (158 kDa), and thyroglobulin (667 kDa). Finally, the fractions containing WSTF and VDR were collected and loaded onto a 2.5–5 ml anti-FLAG M2 resin column (Sigma). After washing with binding buffer, the bound proteins were eluted by incubation for 60 min with 10–15 ml of the FLAG peptide (0.2 mg/ml) (Sigma) in binding buffer.

In Vitro Chromatin Reconstitution and Disruption Assay

Chromatin reconstitution and disruption reactions were performed essentially as previously described (Ito et al., 2000) using supercoiled plasmid DNA. A standard reaction contained plasmid (0.4 μg), purified core histones from *Drosophila* embryos (0.33 μg), purified recombinant dNAP1 (2.8 μg) [dNAP1], purified recombinant ACF (40 ng) [dACF], purified WINAC (100 ng) [WINAC], ATP (3 mM), and the ATP-regenerating system (30 mM phosphocreatine and 1mg/ml creatine phosphokinase). For the chromatin-disruption assay,

chromatin was reconstituted with DNA, pGIE0 (containing the GAL4 binding site) and purified histones by salt dialysis, and GST-GAL4 fusion proteins [e.g., GAL-VDR] mediated disruption of nucleosome arrays was analyzed by micrococcal nuclease digestion-Southern blot analysis.

In Vitro Transcription Assay

The purified proteins were purified as described previously (Ito et al., 2000). An in vitro transcription reactions and primer extension analysis was performed with pGI0 as an internal control, as previously described (Ito et al., 1997). Chromatin was reconstituted with DNA, pGIE0 (0.2 μg), and purified histones (0.24 μg) by salt dialysis and indicated purified GST-GAL4 fusion proteins (50 nM each final concentration), purified WINAC (50 ng) [WINAC] and p300 (40 nM) [p300] were added before the transcription reactions. After primer extension reactions, ^{32}P-labeled DNA was extracted by phenol-chroroform, precipitated by ethanol, analyzed on 8% acrylamide 8.3 M urea gels, and visualized by autoradiography.

In Vitro Replication Assay

An in vitro replication assay was performed as previously described (Ohba et al., 1996). Purified WINAC [WINAC], purified recombinant *Drosophila* NAP-1 [dNAP1], or *Drosophila* CAF-1 [dCAF1] was added before initiating the DNA replication reactions. The products were extracted and subjected to electrophoresis in a 1.5% agarose gel (1 × TBE) and visualized by autoradiography.

Cell Cycle Analysis Using RNAi and DNA Quantity Analysis

For immunoprecipitation during the double-thymidine treatment, about 80% of the confluent cells of FLAG-WSTF stable transformants were treated with thymidine (2.5 mM). After 24 hr, the cells were washed and cultured in normal medium for 10 hr (first release), then were treated with hydroxyurea (1 mM), and cultured for 16 hr (Fujita et al., 1996). Finally, the cells were washed and cultured in normal conditions (final release), then immunoprecipitated with anti-FLAG M2-resin. For the analysis of the DNA histogram, the FACS analysis was done using FACS Calibur (BD PharMingen) and CellQuest (BD PharMingen) (Fujita et al., 1996).

RNAi Experiments

The two short RNAs were transfected after they were annealed. The sequence of the indicated RNAi is as follows: WSTF-RNAi (5′-GAGUAUGAAGCCCGCUUGGTT-3′ and 5′-CCAAGCGGGCUUCAUAC-UCTT-3′); Brg1-RNAi (5′-CUCCUCGGCCAGGUCCUUCTT-3′ and 5′-GAA-GGACCUGGCCGAGGAGTT-3′); Brm-RNAi (5′-UUCUUGGGCCUAGUC-CAGGTT-3′ and 5′-CCUGGACUAGGCCCAAGAATT-3′); CAF-1 p150-RNAi (5′-UCUUGUCCCAAA-GGGGAAATT-3′ and 5′-UUUCCCCUUUGG-GACAAGATT-3′); and control-RNAi (5′-CAGUAAGUAGCCGGGAUGGTT-3′ and 5′-CCAUCCCGGCUACUUA-CUGTT-3′).

ChIP Assay

Preparation of soluble chromatin for PCR amplification was performed as previously reported (Shang et al., 2000; Yanagisawa et al., 2002). The primer pairs for 24(OH)ase were 5′-GGGAGGCGCGTTCGAA-3′ and 5′-TCCTATGCCCAG-GGAC-3′ (pVDRE) and 5′-CCTCCTTTGCACAAGG-TAGT-3′ and 5′-AATGCACGTAAAGCGGCA-AC-3′ (distal); the primers for 1a(OH)ase were 5′-ATTCCCATGTCTGGAAGGAG-3′ and 5′-CAGTGAGC-CCAGCCCCTTTA-3′ (nVDRE) and 5′-AAGCTTGTCTCAACCTCCTG-3′ and 5′-GTTCAGAGATTGTCTGTGGG-3′ (distal).

Acknowledgments

We thank Dr. Michael Jones for kindly providing the partial WSTF cDNAs; Dr. H. Kato and Dr. H. Iba for Brg1 and hBrm plasmids; Dr. J. Kadonaga for dNAP-1; Dr. C. Wu for dACF; Dr. J.K. Tyler for dCAF-1; and Drs. G. Mizuguchi and L. Freedman for technical discussion. We also thank Dr. K. Yamane, H. Kawano, and A. Unno for the technical support; Dr. L. Tora for the critical discussion; and Miss H. Higuchi for preparation of the manuscript. This work was supported in part by a grant-in-aid for priority areas from the Ministry of Education, Science, Sports, and Culture of Japan (S.K.).

Received: December 30, 2002
Revised: May 16, 2003
Accepted: May 28, 2003
Published: June 26, 2003

References

Belandia, B., Orford, R.L., Hurst, H.C., and Parker, M.G. (2002). Targeting of SWI/SNF chromatin remodelling complexes to estrogen-responsive genes. EMBO J. *21*, 4094–4103.

Bozhenok, L., Wade, P.A., and Varga-Weisz, P. (2002). WSTF-ISWI chromatin remodeling complex targets heterochromatic replication foci. EMBO J. *21*, 2231–2241.

Bultman, S., Gebuhr, T., Yee, D., La Mantia, C., Nicholson, J., Gilliam, A., Randazzo, F., Metzger, D., Chambon, P., Crabtree, G., and Magnuson, T. (2000). A Brg1 null mutation in the mouse reveals functional differences among mammalian SWI/SNF complexes. Mol. Cell *6*, 1287–1295.

Chen, K.S., and DeLuca, H.F. (1995). Cloning of the human 1 alpha,25-dihydroxyvitamin D-3 24-hydroxylase gene promoter and identification of two vitamin D-responsive elements. Biochim. Biophys. Acta *1263*, 1–9.

Chiba, H., Muramatsu, M., Nomoto, A., and Kato, H. (1994). Two human homologues of Saccharomyces cerevisiae SWI2/SNF2 and Drosophila brahma are transcriptional coactivators cooperating with the estrogen receptor and the retinoic acid receptor. Nucleic Acids Res. *22*, 1815–1820.

DiRenzo, J., Shang, Y., Phelan, M., Sif, S., Myers, M., Kingston, R., and Brown, M. (2000). BRG-1 is recruited to estrogen-responsive promoters and cooperates with factors involved in histone acetylation. Mol. Cell. Biol. *20*, 7541–7549.

Elbashir, S.M., Harborth, J., Lendeckel, W., Yalcin, A., Weber, K., and Tuschl, T. (2001). Duplexes of 21-nucleotide RNAs mediate RNA interference in cultured mammalian cells. Nature *411*, 494–498.

Emerson, B.M. (2002). Specificity of gene regulation. Cell *109*, 267–270.

Fujita, M., Kiyono, T., Hayashi, Y., and Ishibashi, M. (1996). hCDC47, a human member of the MCM family. Dissociation of the nucleus-bound form during S phase. J. Biol. Chem. *271*, 4349–4354.

Fyodorov, D.V., and Kadonaga, J.T. (2001). The many faces of chromatin remodeling: SWItching beyond transcription. Cell *106*, 523–525.

Fyodorov, D.V., and Kadonaga, J.T. (2002). Binding of Acf1 to DNA involves a WAC motif and is important for ACF-mediated chromatin assembly. Mol. Cell. Biol. *22*, 6344–6353.

Garabedian, M., Jacqz, E., Guillozo, H., Grimberg, R., Guillot, M., Gagnadoux, M.F., Broyer, M., Lenoir, G., and Balsan, S. (1985). Elevated plasma 1,25-dihydroxyvitamin D concentrations in infants with hypercalcemia and an elfin facies. N. Engl. J. Med. *312*, 948–952.

Glass, C.K., and Rosenfeld, M.G. (2000). The coregulator exchange in transcriptional functions of nuclear receptors. Genes Dev. *14*, 121–141.

Gu, W., Malik, S., Ito, M., Yuan, C.X., Fondell, J.D., Zhang, X., Martinez, E., Qin, J., and Roeder, R.G. (1999). A novel human SRB/MED-containing cofactor complex, SMCC, involved in transcription regulation. Mol. Cell *3*, 97–108.

Hassan, A.H., Prochasson, P., Neely, K.E., Galasinski, S.C., Chandy, M., Carrozza, M.J., and Workman, J.L. (2002). Function and selectivity of bromodomains in anchoring chromatin-modifying complexes to promoter nucleosomes. Cell *111*, 369–379.

Hoogenraad, C.C., Koekkoek, B., Akhmanova, A., Krugers, H., Dortland, B., Miedema, M., van Alphen, A., Kistler, W.M., Jaegle, M., Koutsourakis, M., et al. (2002). Targeted mutation of Cyln2 in the Williams syndrome critical region links CLIP-115 haploinsufficiency to neurodevelopmental abnormalities in mice. Nat. Genet. *32*, 116–127.

Ito, T., Bulger, M., Pazin, M.J., Kobayashi, R., and Kadonaga, J.T. (1997). ACF, an ISWI-containing and ATP-utilizing chromatin assembly and remodeling factor. Cell *90*, 145–155.

Ito, T., Ikehara, T., Nakagawa, T., Kraus, W.L., and Muramatsu, M. (2000). p300-mediated acetylation facilitates the transfer of histone H2A–H2B dimers from nucleosomes to a histone chaperone. Genes Dev. *14*, 1899–1907.

Jones, M.H., Hamana, N., Nezu, J., and Shimane, M. (2000). A novel family of bromodomain genes. Genomics *63*, 40–45.

Kamei, Y., Xu, L., Heinzel, T., Torchia, J., Kurokawa, R., Gloss, B., Lin, S.C., Heyman, R.A., Rose, D.W., Glass, C.K., and Rosenfeld, M.G. (1996). A CBP integrator complex mediates transcriptional activation and AP-1 inhibition by nuclear receptors. Cell *85*, 403–414.

Kim, J.K., Huh, S.O., Choi, H., Lee, K.S., Shin, D., Lee, C., Nam, J.S., Kim, H., Chung, H., Lee, H.W., et al. (2001). Srg3, a mouse homolog of yeast SWI3, is essential for early embryogenesis and involved in brain development. Mol. Cell. Biol. *21*, 7787–7795.

Kitagawa, H., Yanagisawa, J., Fuse, H., Ogawa, S., Yogiashi, Y., Okuno, A., Nagasawa, H., Nakajima, T., Matsumoto, T., and Kato, S. (2002). Ligand-selective potentiation of rat mineralocorticoid receptor activation function 1 by a CBP-containing histone acetyltransferase complex. Mol. Cell. Biol. *22*, 3698–3706.

Lazzaro, M.A., and Picketts, D.J. (2001). Cloning and characterization of the murine imitation switch (ISWI) genes: differential expression patterns suggest distinct developmental roles for Snf2h and Snf2l. J. Neurochem. *77*, 1145–1156.

Lemon, B., Inouye, C., King, D.S., and Tjian, R. (2001). Selectivity of chromatin-remodelling cofactors for ligand-activated transcription. Nature *414*, 924–928.

LeRoy, G., Orphanides, G., Lane, W.S., and Reinberg, D. (1998). Requirement of RSF and FACT for transcription of chromatin templates in vitro. Science *282*, 1900–1904.

Lomvardas, S., and Thanos, D. (2002). Modifying gene expression programs by altering core promoter chromatin architecture. Cell *110*, 261–271.

Loyola, A., LeRoy, G., Wang, Y.H., and Reinberg, D. (2001). Reconstitution of recombinant chromatin establishes a requirement for histone-tail modifications during chromatin assembly and transcription. Genes Dev. *15*, 2837–2851.

Lu, X., Meng, X., Morris, C.A., and Keating, M.T. (1998). A novel human gene, WSTF, is deleted in Williams syndrome. Genomics *54*, 241–249.

Mangelsdorf, D.J., Thummel, C., Beato, M., Herrlich, P., Schutz, G., Umesono, K., Blumberg, B., Kastner, P., Mark, M., Chambon, P., et al. (1995). The nuclear receptor superfamily: the second decade. Cell *83*, 835–839.

Murayama, A., Takeyama, K., Kitanaka, S., Kodera, Y., Hosoya, T., and Kato, S. (1998). The promoter of the human 25-hydroxyvitamin D3 1 alpha-hydroxylase gene confers positive and negative responsiveness to PTH, calcitonin, and 1 alpha,25(OH)2D3. Biochem. Biophys. Res. Commun. *249*, 11–16.

Narlikar, G.J., Fan, H.Y., and Kingston, R.E. (2002). Cooperation between complexes that regulate chromatin structure and transcription. Cell *108*, 475–487.

Ohba, R., Matsumoto, K., and Ishimi, Y. (1996). Induction of DNA replication by transcription in the region upstream of the human c-myc gene in a model replication system. Mol. Cell. Biol. *16*, 5754–5763.

Onate, S.A., Tsai, S.Y., Tsai, M.J., and O'Malley, B.W. (1995). Sequence and characterization of a coactivator for the steroid hormone receptor superfamily. Science *270*, 1354–1357.

Peoples, R.J., Cisco, M.J., Kaplan, P., and Francke, U. (1998). Identification of the WBSCR9 gene, encoding a novel transcriptional regulator, in the Williams-Beuren syndrome deletion at 7q11.23. Cytogenet. Cell Genet. *82*, 238–246.

Poot, R.A., Dellaire, G., Hulsmann, B.B., Grimaldi, M.A., Corona, D.F., Becker, P.B., Bickmore, W.A., and Varga-Weisz, P.D. (2000). HuCHRAC, a human ISWI chromatin remodelling complex contains hACF1 and two novel histone-fold proteins. EMBO J. *19*, 3377–3387.

Rachez, C., Suldan, Z., Ward, J., Chang, C.P., Burakov, D., Erdjument-Bromage, H., Tempst, P., and Freedman, L.P. (1998). A novel protein complex that interacts with the vitamin D3 receptor in a ligand-dependent manner and enhances VDR transactivation in a cell-free system. Genes Dev. *12*, 1787–1800.

Schultz, D.C., Ayyanathan, K., Negorev, D., Maul, G.G., and Rauscher, F.J., 3rd. (2002). SETDB1: a novel KAP-1-associated histone H3, lysine 9-specific methyltransferase that contributes to HP1-mediated silencing of euchromatic genes by KRAB zinc-finger proteins. Genes Dev. *16*, 919–932.

Sekine, K., Ohuchi, H., Fujiwara, M., Yamasaki, M., Yoshizawa, T., Sato, T., Yagishita, N., Matsui, D., Koga, Y., Itoh, N., and Kato, S. (1999). Fgf10 is essential for limb and lung formation. Nat. Genet. *21*, 138–141.

Shang, Y., Hu, X., DiRenzo, J., Lazar, M.A., and Brown, M. (2000). Cofactor dynamics and sufficiency in estrogen receptor-regulated transcription. Cell *103*, 843–852.

Shang, Y., Myers, M., and Brown, M. (2002). Formation of the androgen receptor transcription complex. Mol. Cell *9*, 601–610.

Smith, S., and Stillman, B. (1989). Purification and characterization of CAF-I, a human cell factor required for chromatin assembly during DNA replication in vitro. Cell *58*, 15–25.

Soutoglou, E., and Talianidis, I. (2002). Coordination of PIC assembly and chromatin remodeling during differentiation-induced gene activation. Science *295*, 1901–1904.

Taylor, A.B., Stern, P.H., and Bell, N.H. (1982). Abnormal regulation of circulating 25-hydroxyvitamin D in the Williams syndrome. N. Engl. J. Med. *306*, 972–975.

Varga-Weisz, P.D., Wilm, M., Bonte, E., Dumas, K., Mann, M., and Becker, P.B. (1997). Chromatin-remodelling factor CHRAC contains the ATPases ISWI and topoisomerase II. Nature *388*, 598–602.

Yanagisawa, J., Kitagawa, H., Yanagida, M., Wada, O., Ogawa, S., Nakagomi, M., Oishi, H., Yamamoto, Y., Nagasawa, H., McMahon, S.B., et al. (2002). Nuclear receptor function requires a TFTC-type histone acetyl transferase complex. Mol. Cell *9*, 553–562.

Yasui, D., Miyano, M., Cai, S., Varga-Weisz, P., and Kohwi-Shigematsu, T. (2002). SATB1 targets chromatin remodelling to regulate genes over long distances. Nature *419*, 641–645.

Yoshizawa, T., Handa, Y., Uematsu, Y., Takeda, S., Sekine, K., Yoshihara, Y., Kawakami, T., Arioka, K., Sato, H., Uchiyama, Y., et al. (1997). Mice lacking the vitamin D receptor exhibit impaired bone formation, uterine hypoplasia and growth retardation after weaning. Nat. Genet. *16*, 391–396.

AC, Santa Cruz) for immunoprecipitation; a monoclonal antibody against haemagglutinin A (HA; 1867423, Roche), a polyclonal antibody against Myc (SC789, Santa Cruz), and antibodies against phosphylated (Ser 473) or total Akt (9270, New England Biolabs).

Statistical analysis

Results shown are the mean ± s.d. We analysed data by one-way analysis of variance (ANOVA). Individual statistical differences were determined by Scheffe's multiple range comparison test.

Accession numbers

The sequences of mouse and human ERas can be retrieved from DDBJ/GenBank/EMBL with accession numbers AB093573 and AB093575.

Received 10 February; accepted 1 April 2003; doi:10.1038/nature01646.

1. Evans, M. J. & Kaufman, M. H. Establishment in culture of pluripotential cells from mouse embryos. *Nature* **292,** 154–156 (1981).
2. Martin, G. R. Isolation of a pluripotent cell line from early mouse embryos cultured in medium conditioned by teratocarcinoma stem cells. *Proc. Natl Acad. Sci. USA* **78,** 7634–7638 (1981).
3. Thomson, J. A. *et al.* Embryonic stem cell lines derived from human blastocysts. *Science* **282,** 1145–1147 (1998).
4. Freed, C. R. Will embryonic stem cells be a useful source of dopamine neurons for transplant into patients with Parkinson's disease? *Proc. Natl Acad. Sci. USA* **99,** 1755–1757 (2002).
5. Seeburg, P. H., Colby, W. W., Capon, D. J., Goeddel, D. V. & Levinson, A. D. Biological properties of human c-*Ha-ras1* genes mutated at codon 12. *Nature* **312,** 71–75 (1984).
6. Rodriguez-Viciana, P. *et al.* Phosphatidylinositol-3-OH kinase as a direct target of Ras. *Nature* **370,** 527–532 (1994).
7. Moodie, S. A., Willumsen, B. M., Weber, M. J. & Wolfman, A. Complexes of Ras.GTP with Raf-1 and mitogen-activated protein kinase kinase. *Science* **260,** 1658–1661 (1993).
8. Zhang, X. F. *et al.* Normal and oncogenic p21^{ras} proteins bind to the amino-terminal regulatory domain of c-Raf-1. *Nature* **364,** 308–313 (1993).
9. Takai, Y., Sasaki, T. & Matozaki, T. Small GTP-binding proteins. *Physiol. Rev.* **81,** 153–208 (2001).
10. Chen, Z. Q., Ulsh, L. S., DuBois, G. & Shih, T. Y. Posttranslational processing of p21 ras proteins involves palmitylation of the C-terminal tetrapeptide containing cysteine-186. *J. Virol.* **56,** 607–612 (1985).
11. Willumsen, B. M., Christensen, A., Hubbert, N. L., Papageorge, A. G. & Lowy, D. R. The p21 ras C-terminus is required for transformation and membrane association. *Nature* **310,** 583–586 (1984).
12. Miyoshi, J., Kagimoto, M., Soeda, E. & Sakaki, Y. The human c-*Ha-ras2* is a processed pseudogene inactivated by numerous base substitutions. *Nucleic Acids Res.* **12,** 1821–1828 (1984).
13. Meiner, V. L. *et al.* Disruption of the acyl-CoA:cholesterol acyltransferase gene in mice: evidence suggesting multiple cholesterol esterification enzymes in mammals. *Proc. Natl Acad. Sci. USA* **93,** 14041–14046 (1996).
14. Li, E., Bestor, T. H. & Jaenisch, R. Targeted mutation of the DNA methyltransferase gene results in embryonic lethality. *Cell* **69,** 915–926 (1992).
15. Nichols, J., Evans, E. P. & Smith, A. G. Establishment of germ-line-competent embryonic stem (ES) cells using differentiation inhibiting activity. *Development* **110,** 1341–1348 (1990).
16. Gassmann, M., Donoho, G. & Berg, P. Maintenance of an extrachromosomal plasmid vector in mouse embryonic stem cells. *Proc. Natl Acad. Sci. USA* **92,** 1292–1296 (1995).
17. Fasano, O. *et al.* Analysis of the transforming potential of the human H-ras gene by random mutagenesis. *Proc. Natl Acad. Sci. USA* **81,** 4008–4012 (1984).
18. Serrano, M., Lin, A. W., McCurrach, M. E., Beach, D. & Lowe, S. W. Oncogenic *ras* provokes premature cell senescence associated with accumulation of p53 and p16^{INK4a}. *Cell* **88,** 593–602 (1997).
19. Cheng, A. M. *et al.* Mammalian Grb2 regulates multiple steps in embryonic development and malignant transformation. *Cell* **95,** 793–803 (1998).
20. Burdon, T., Stracey, C., Chambers, I., Nichols, J. & Smith, A. Suppression of SHP-2 and ERK signalling promotes self-renewal of mouse embryonic stem cells. *Dev. Biol.* **210,** 30–43 (1999).
21. Rodriguez-Viciana, P. *et al.* Role of phosphoinositide 3-OH kinase in cell transformation and control of the actin cytoskeleton by Ras. *Cell* **89,** 457–467 (1997).
22. Di Cristofano, A., Pesce, B., Cordon-Cardo, C. & Pandolfi, P. P. Pten is essential for embryonic development and tumour suppression. *Nature Genet.* **19,** 348–355 (1998).
23. Sun, H. *et al.* PTEN modulates cell cycle progression and cell survival by regulating phosphatidylinositol 3,4,5-trisphosphate and Akt/protein kinase B signaling pathway. *Proc. Natl Acad. Sci. USA* **96,** 6199–6204 (1999).
24. Burgering, B. M. & Coffer, P. J. Protein kinase B (c-Akt) in phosphatidylinositol-3-OH kinase signal transduction. *Nature* **376,** 599–602 (1995).
25. Franke, T. F. *et al.* The protein kinase encoded by the Akt proto-oncogene is a target of the PDGF-activated phosphatidylinositol 3-kinase. *Cell* **81,** 727–736 (1995).
26. Klippel, A. *et al.* Membrane localization of phosphatidylinositol 3-kinase is sufficient to activate multiple signal-transducing kinase pathways. *Mol. Cell. Biol.* **16,** 4117–4127 (1996).
27. Jirmanova, I., Afanassieff, M., Gobert-Gosse, S., Markossian, S. & Savatier, P. Differential contributions of ERK and PI3-kinase to the regulation of cyclin D1 expression and to the control of the G1/S transition in mouse embryonic stem cells. *Oncogene* **21,** 5515–5528 (2002).
28. Quilliam, L. A. M.-R. *et al.* Ras/R-Ras3, a transforming ras protein regulated by Sos1, GRF1, and p120 Ras GTPase-activating protein, interacts with the putative Ras effector AF6. *J. Biol. Chem.* **274,** 23850–23857 (1999).
29. Clark, G. J., Cox, A. D., Graham, S. M. & Der, C. J. Biological assays for Ras transformation. *Methods Enzymol.* **255,** 395–412 (1995).
30. Rosario, M., Paterson, H. F. & Marshall, C. J. Activation of the Raf/MAP kinase cascade by the Ras-related protein TC21 is required for the TC21-mediated transformation of NIH 3T3 cells. *EMBO J.* **18,** 1270–1279 (1999).

Supplementary Information accompanies the paper on **www.nature.com/nature.**

Acknowledgements We thank E. Kaiho, Y. Tokuzawa and M. Murakami for discussion; C. Takigawa and J. Iida for technical assistance; T. Ichisaka and Y. Samitsu for blastocyst microinjection; R. Farese Jr for RF8 ES cells, R. Jaenisch and T. Noda for J1 cells; W. Skarnes and S. Young for CGR8 cells; H. Niwa for MG1.19 cells, pCAG-IP and pBIKS(−)BgeopA; M. Okabe and J.-i. Miyazaki for pCX–EGFP; K. Kohno and T. Kitamura for PLAT-E cells and pMX retroviral vectors; and S. Young, R. Farese Jr and R. Pitas for critically reading the manuscript.

Competing interests statement The authors declare that they have no competing financial interests.

Correspondence and requests for materials should be addressed to S.Y. (shinyay@gtc.aist-nara.ac.jp).

Modulation of oestrogen receptor signalling by association with the activated dioxin receptor

Fumiaki Ohtake*, Ken-ichi Takeyama*†, Takahiro Matsumoto*, Hirochika Kitagawa*, Yasuji Yamamoto‡, Keiko Nohara§‖, Chiharu Tohyama§‖, Andree Krust¶, Junsei Mimura‖#, Pierre Chambon¶, Junn Yanagisawa*†, Yoshiaki Fujii-Kuriyama‖# & Shigeaki Kato*†

* *The Institute of Molecular and Cellular Biosciences, University of Tokyo, 1-1-1 Yayoi, Bunkyo-ku, Tokyo, 113-0032, Japan*
† *SORST, Japan Science and Technology, Kawaguchi, Saitama 332-0012, Japan*
‡ *Taiho Pharmaceutical Company Ltd, Cancer Research Laboratory, Hanno Research Center, Hanno, Saitama, 357-8527, Japan*
§ *National Institute for Environmental Studies, Tsukuba, Ibaraki 305-8506, Japan*
‖ *CREST, Japan Science and Technology, Kawaguchi, Saitama 332-0012, Japan*
¶ *Institut de Génétique et de Biologie Moleculaire et Cellulaire, CNRS, INSERM, Université Louis Pasteur, Collège de France, 67404 Illkirch, Strasbourg, France*
\# *TARA Center, University of Tsukuba, Tennodai, Tsukuba, 305-8577, Japan*

Environmental contaminants affect a wide variety of biological events in many species. Dioxins are typical environmental contaminants that exert adverse oestrogen-related effects[1]. Although their anti-oestrogenic actions[2,3] are well described, dioxins can also induce endometriosis[4–7] and oestrogen-dependent tumours[8,9], implying possible oestrogenic effects. However, the molecular mechanism underlying oestrogen-related actions of dioxins remains largely unknown. A heterodimer of the dioxin receptor (AhR) and Arnt, which are basic helix–loop–helix/PAS-family transcription factors, mediates most of the toxic effects of dioxins[10,11]. Here we show that the agonist-activated AhR/Arnt heterodimer directly associates with oestrogen receptors ER-α and ER-β. This association results in the recruitment of unliganded ER and the co-activator p300 to oestrogen-responsive gene promoters, leading to activation of transcription and oestrogenic effects. The function of liganded ER is attenuated. Oestrogenic actions of AhR agonists were detected in wild-type ovariectomized mouse uteri, but were absent in AhR$^{-/-}$ or ER-α$^{-/-}$ ovariectomized mice. Our findings suggest a novel mechanism by which ER-mediated oestrogen signalling is modulated by a co-regulatory-like function of activated AhR/Arnt, giving rise to adverse oestrogen-related actions of dioxin-type environmental contaminants.

ERs, which are members of the nuclear receptor (NR) family[12,13], and AhR/Arnt are both ligand-dependent transcription factors. Ligand-activated AhR heterodimerizes with Arnt and activates the transcription of dioxin target genes such as *CYP1A1* (refs 10,11) through xenobiotic response elements (XREs). ERs bind to oestrogen response elements (EREs) and activate transcription in an oestrogen-dependent manner. This transcriptional activation

requires the recruitment of co-activator complexes[13–18], including histone acetyltransferase (HAT) complexes containing p300 and CREB binding protein (CBP). In view of previous reports that AhR ligands exhibit oestrogen-related adverse effects, it is possible that ER-mediated oestrogen signalling might cross-talk with AhR-mediated signalling through an unknown mechanism that regulates transcription. We therefore decided to examine whether AhR/Arnt heterodimer could transcriptionally affect ER transactivation functions, thereby modulating oestrogen signalling.

To monitor the transactivation function of endogenous receptors, luciferase reporter plasmids bearing consensus binding elements—ERE for ERs, and XRE for AhR/Arnt—were transfected into MCF-7 cells, a breast cancer cell line known to express both receptors endogenously[2]. Although the synthetic AhR ligand 3-methylcholanthrene (3MC) effectively activated transcription through XRE[10], 17β-estradiol (E2) did not, as expected (Fig. 1a). However, to our surprise, 3MC alone activated ERE-mediated transcription in the absence of E2 (Fig. 1a). In the presence of E2, ERE-mediated transcription was decreased by the addition of 3MC. Western blotting showed that the amount of ligand-induced transactivation did not simply reflect variations in receptor numbers (Fig. 1a). 3MC alone decreased AhR and ER-α protein levels, in agreement with previous reports[19].

We then examined the effect of AhR/Arnt on ER-mediated transcription by using exogenous receptors in Ishikawa cells, a uterine tumour cell line. Again, 3MC potently stimulated ERE-mediated transcription in the absence of E2 when both ER (either ER-α or ER-β) and AhR/Arnt were expressed, whereas it lowered the E2-induced transactivation function of ERs (Fig. 1b) without binding directly to ERs (Supplementary Fig. 1a) or affecting expression levels of ERs (data not shown). This activation effect of 3MC requires ERE (Fig. 1b, lanes 1–4), ER-α (lanes 7 and 8), AhR (lanes 9 and 10) and Arnt (lanes 11 and 12). To verify that an AhR ligand does indeed exert oestrogenic action through direct binding to AhR, other AhR ligands were further tested. More stable ligands such as 2,3,7,8-tetrachlorodibenzo-*p*-dioxin (TCDD), benzo[*a*]-pyrene and β-naphthoflavone acted as agonists, like 3MC (Fig. 1c), whereas the oestrogenic action of 3MC was blocked by either a known AhR antagonist, α-naphthoflavone or a pure oestrogen antagonist, ICI182,780 (Fig. 1d). The modulation of transcription activity by AhR/Arnt observed with ERs was not detected on other NRs including glucocorticoid receptor, progesterone receptor, vitamin D receptor (VDR), retinoic acid receptor and peroxisome proliferator activated receptor-γ (PPAR-γ) (data not shown).

Because ERs possess two transactivation functions, AF-1 and AF-2, in the amino-terminal A/B and carboxy-terminal E/F regions, respectively[16,20], we examined the functional association of AhR/Arnt with these two regions using ER deletion mutants (HE15 for AF-1 domain, and HE19 for AF-2 domain) (Supplementary Fig. 1b) in Ishikawa cells. The N-terminal A/B regions of ER-α and ER-β were required for stimulation of ERE-mediated transcription by AhR/Arnt, whereas we detected no modulation of AF-2 functions (Fig. 1e)[20]. Thus, 3MC-bound AhR/Arnt might modulate the functions of ERs through association with the N-terminal A/B regions. This possibility was supported by the observation that

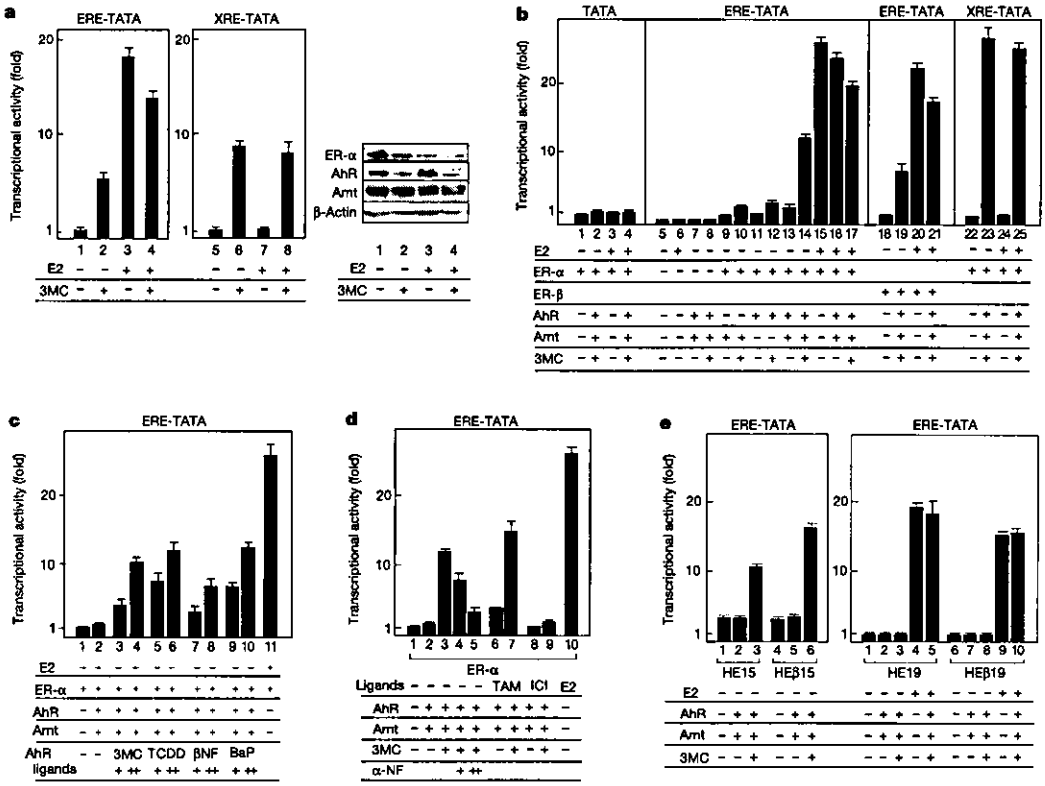

Figure 1 Activation of unliganded ER function by liganded dioxin receptor heterodimer. **a**, A dioxin receptor ligand activates transcription mediated through an ERE. MCF-7 cells were transfected with the reporter plasmids ERE-luciferase or XRE-luciferase in the presence or absence of E2 (10 nM) and 3MC (1 μM). Luciferase assays were performed with the cell extracts. All values are means ± s.d. for at least three independent experiments. **b**, Liganded AhR/Arnt induces the transactivation function of ERE-bound unliganded ER. Ishikawa cells transfected with the indicated plasmids were subjected to luciferase assays. **c**, Transactivation of unliganded ER by the other AhR agonists. **d**, Potentiation of ERE-mediated transcription by liganded AhR/Arnt is blocked by an antagonist for either ER-α or AhR. Cells treated with tamoxifen (TAM; 100 nM), ICI182,780 (ICI; 100 nM), 3MC (+, 100 nM; ++, 1 μM), TCDD (+, 10 nM; ++, 100 nM), β-naphthoflavone (β-NF; +, 100 nM; ++, 1 μM), benzo[*a*]pyrene (BaP; +, 10 nM; ++, 100 nM), α-naphthoflavone (α-NF; +, 100 nM; ++,1 μM). **e**, Potentiation of ERE-mediated transcription by AhR/Arnt is mediated by the ERs A/B regions.

3MC-bound AhR/Arnt potentiates the transactivation function of ER-α in the presence of the ER-α AF-1 agonist/AF-2 antagonist tamoxifen (Fig. 1d)[16].

We then tested whether a 3MC-dependent physical interaction occurred between AhR/Arnt and ERs. Irrespective of E2 binding, endogenous ER-α in MCF-7 cells, and tagged ER-α overexpressed in COS-1 cells, were found to co-immunoprecipitate with 3MC-bound AhR, but not with unliganded AhR, only when Arnt was co-expressed (Fig. 2a and b). In agreement with the functional interaction between AhR/Arnt and the A/B region of ER-α (Fig. 1e), a 3MC-dependent interaction between AhR/Arnt and HE15 was observed, but not between AhR/Arnt and HE19 (ref. 12). Although ER-β, like ER-α, also associated with AhR in a 3MC-dependent fashion, no other receptors tested showed such an association (Fig. 2b).

Moreover, a direct interaction between AhR, but not Arnt, and A/B regions from both ER-α and ER-β could be mapped by an *in vitro* glutathione *S*-transferase (GST) pull-down assay (Fig. 2c). It therefore seems that, upon ligand binding and nuclear translocation[10], AhR heterodimerizes with nuclear Arnt and then associates with unliganded ER-α or ER-β, which are constitutively in the nucleus[16], through direct interaction with their A/B regions. Further analyses by GST pull-down assay mapped the small regions of the A/B region of ER-α (residues 40–120), the A/B region of ER-β (residues 33–55)[21], and the helix–loop–helix/PAS domain of AhR[22], which are indispensable for direct interaction *in vitro* (Fig. 2d and Supplementary Fig. 2a). An ER-α mutant lacking the AhR-interacting region (ER-α ΔAhR) failed to be activated by AhR/Arnt but responsiveness to E2 was still retained, supporting the idea that the interaction is required for AhR ligand-induced activation of the ER function (Fig. 2e).

To explore the molecular mechanisms of the 3MC-dependent transactivation function of AhR and ERs, we used co-immunoprecipitation to examine whether p300 was recruited to the complex, because both AhR and ERs have been independently reported to require p300/CRB as a co-activator[10,16,18,23]. p300 was recruited to ER-α in the presence but not the absence of E2 (Fig. 2f, lanes 2 and 4). However, even in the absence of E2, p300 associated with 3MC-bound AhR/Arnt and unliganded ER-α to form a complex (Fig. 2f, lane 3). Recruitment of the p160 family co-activator SRC-1 (ref. 13; Fig. 2f, lane 3), TIF2 or AIB1 (data not shown) to AhR/Arnt-associated ERs were not detected. Thus, the co-activator complex required to activate transcription by the unliganded ERs associated with liganded AhR/Arnt might be distinct from both co-activator

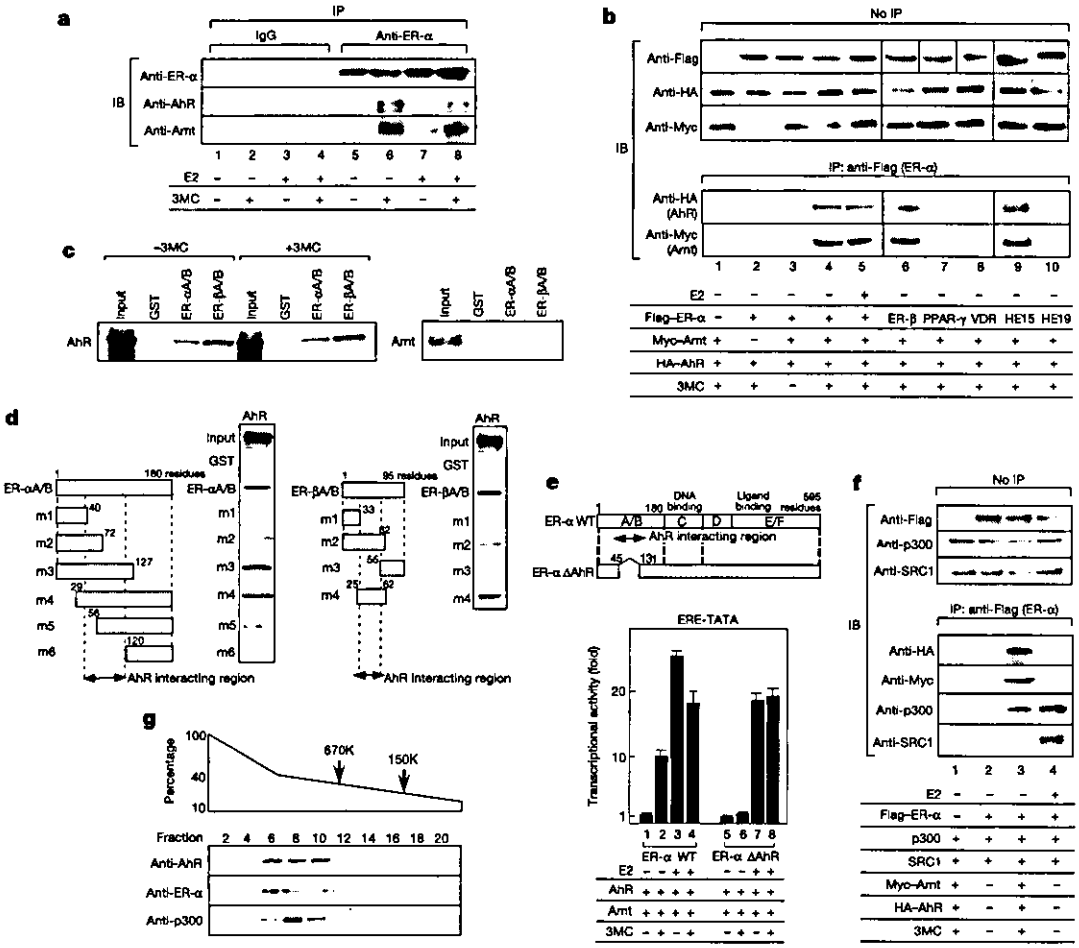

Figure 2 3MC-dependent interaction of ERs with AhR/Arnt. **a**, 3MC-dependent but E2-independent interaction of endogenous ER-α with AhR/Arnt in MCF-7 cells. Cells were subjected to immunoprecipitation (IP) with mouse anti-ER-α or normal mouse immunoglobulin as a control. The immunoprecipitates were western blotted (IB) with specific antibodies as indicated. **b**, E2-independent, 3MC-dependent interaction of exogenous ERs with AhR/Arnt in COS-1 cells. The transfected cells were subjected to immunoprecipitation and then western blotting. PPAR, peroxisomeproliferatoractivated receptor; VDR, vitamin D receptor. **c**, Direct but 3MC-independent interaction of AhR with ER-α and ER-β in an *in vitro* GST pull-down assay. **d**, Mapping the interaction domains of ER-α and ER-β with AhR. **e**, The AhR-interacting core region in the ER-α A/B domain is required for ER-α activation by AhR/Arnt. Luciferase assays with the indicated ER derivative. **f**, Recruitment of p300 co-activator to a complex containing unliganded ER-α and 3MC-bound AhR/Arnt. **g**, AhR/ER–α/p300 form a complex on glycerol gradient analysis. The Flag–AhR associated proteins in stable transformant HeLa cells were fractionated by molecular mass by a glycerol gradient assay.

complexes for the unassociated receptors. Indeed, ER-α and p300 were detected in the same fractions as Flag ($[EYKEEEK]_2$)-tagged AhR fractionated by a glycerol gradient, suggesting that they form a complex with a relative molecular mass (M_r) larger than 670,000 (670K) (Fig. 2g).

To investigate whether the observed association between AhR and ERs occurred on EREs in endogenous target gene promoters of MCF-7 cells, we performed a chromatin immunoprecipitation (ChIP) analysis with *pS2* and *c-fos* gene promoters[17]. Interestingly, 3MC induced binding of ER-α to ERE, as did E2, with AhR/Arnt recruitment. As expected, 3MC induced the recruitment of AhR/Arnt, but not ER-α, to the *CYP1A1* promoter XRE (Fig. 3a). Reflecting the recruitment of the receptors, acetylation of histone H4 was observed in the promoters (Fig. 3a), indicating the possible recruitment of a HAT co-activator complex to the receptors. The expression of these genes was accordingly induced by 3MC or E2 (Fig. 3d). Thus, the 3MC-dependent association between AhR/Arnt and ER-α seems to promote the binding of unliganded ER-α to EREs.

A ChIP assay involving sequential immunoprecipitation confirmed the 3MC-dependent association of AhR/Arnt with ER-α on

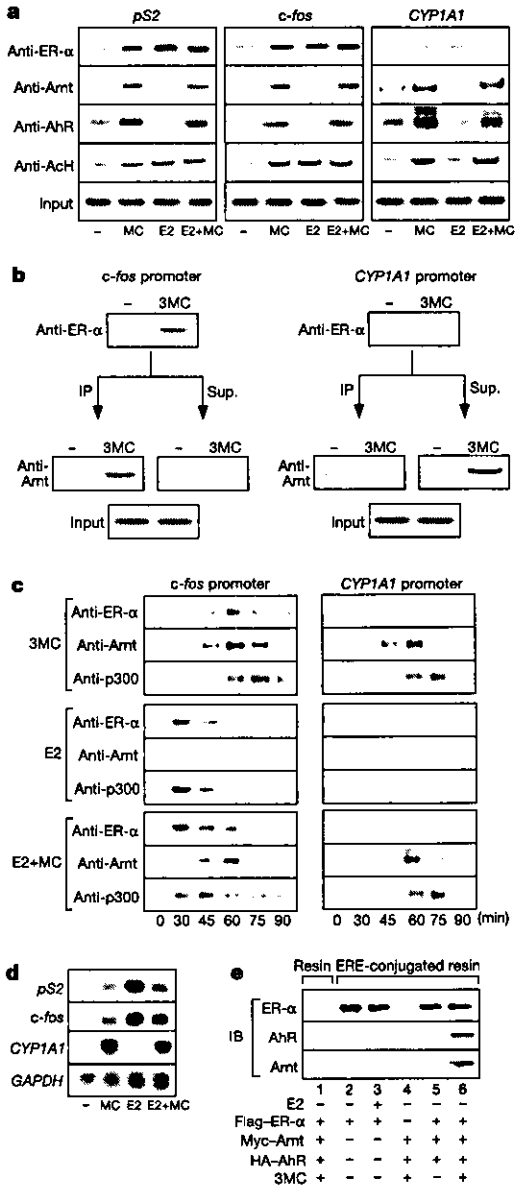

Figure 3 3MC-dependent recruitment of AhR/Arnt to ER-α bound on oestrogen-responsive gene promoters. **a**, 3MC-dependent interaction with AhR/Arnt induces ERE binding of unliganded ER-α to E2 responsive gene promoters in MCF-7 cells. For ChIP analyses, soluble chromatin prepared from MCF-7 cells treated with ligands for 45 min was immunoprecipitated with the indicated antibodies. The final DNA extracts were amplified using specific sets of primer pairs to detect the c-*fos*, *pS2* and *CYP1A1* gene promoters as indicated. **b**, 3MC-dependent association of AhR/Arnt with ER-α bound to E2-responsive gene promoters. The immunoprecipitates and their supernatants were sequentially applied for ChIP analysis as indicated. **c**, Dynamics of ER-α–Arnt–p300 assembly on ligand-responsive gene promoters. Occupancy of the c-*fos* and *CYP1A1* promoters by ER-α, Arnt and p300 at different times after ligand treatments. **d**, Induction of target genes examined by northern blot analysis. **e**, Complex formation of AhR–Arnt–ER-α on ERE through ER-α as revealed by ABCD assay.

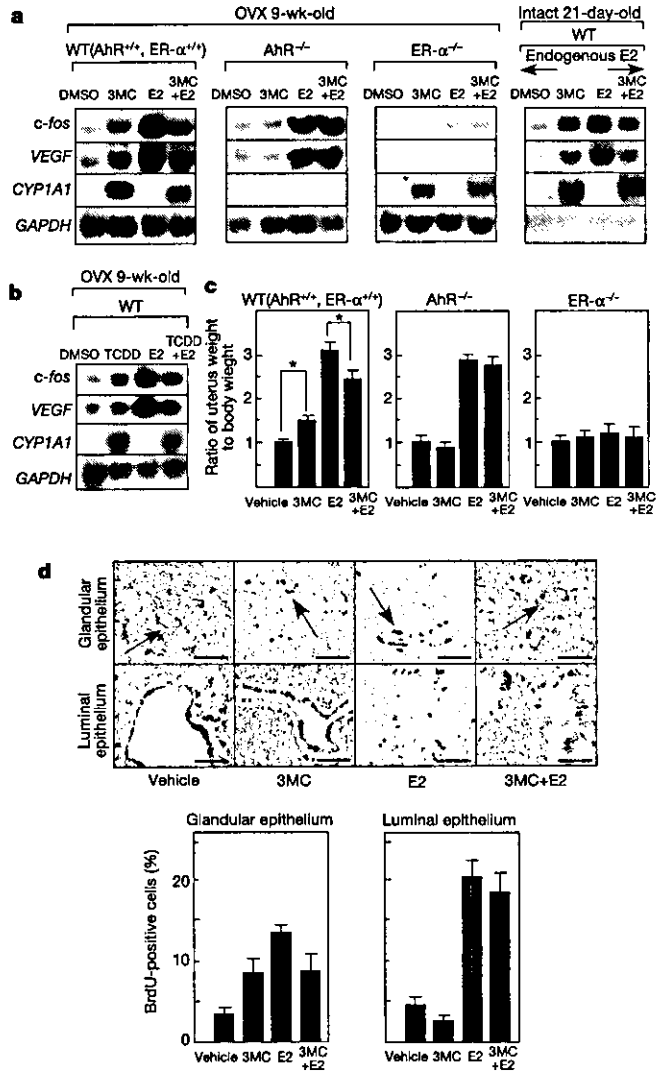

Figure 4 Oestrogenic actions of 3MC in mouse uterus are mediated by AhR and ER-α. **a**, **b**, Induction of E2-responsive genes by AhR agonists is mediated by both AhR and ER-α. Nine-week-old ovariectomized (OVX) mice and intact 21-day-old female mice of the indicated genotypes were injected with the ligands. Three hours later, total RNA was extracted from the uterus, then subjected to northern blot analysis with cDNAs for the target genes for E2 (c-*fos*, *VEGF*) and for 3MC (*CYP1A1*); *GAPDH* cDNA was used as an internal control. WT, wild type. **c**, The 3MC-induced increase in uterine wet weight (measured as the ratio of uterine wet weight in milligrams to body weight in grams) in ovariectomized mice was abolished by inactivation by either AhR or ER-α. The *t*-test shows a significant difference ($P < 0.01$) between 3MC-treated ($n = 9$) and olive-oil-treated ($n = 9$) wild-type mice. There is no significant difference ($P > 0.2$) between 3MC-treated ($n = 4$) and olive-oil-treated ($n = 4$) animals in either $AhR^{-/-}$ and $ER\text{-}\alpha^{-/-}$ mice. All values are means ± s.e.m. **d**, Induction of endometrial cell proliferation by 3MC and E2. BrdU-positive cells (brown) are indicated by arrows.

ERE (Fig. 3b). A time-course ChIP assay showed that ER-α, AhR and p300 HAT were simultaneously recruited to the c-*fos* promoter, presumably upon the binding of 3MC to AhR (Fig. 3c).

To verify the interaction of AhR/Arnt with ER-α bound to ERE in the promoters, the formation of a complex with ERE was tested by avidin–biotin-conjugated DNA(ERE) (ABCD) precipitation[24] (Fig. 3e). ER-α bound to consensus ERE (Fig. 3e, lanes 2, 3, 5 and 6), whereas AhR/Arnt alone did not (Fig. 3e, lane 4). However, in the presence of ER-α, AhR/Arnt was recruited to ERE in a 3MC-dependent manner (Fig. 3e, lanes 5 and 6). In the transient luciferase assay, the binding of ER-α to ERE and the activation function of both AhR and Arnt were required for the activation of ER-α through ERE by AhR/Arnt (Supplementary Fig. 3a, lanes 3, 7, and 8), whereas the AF-1 and AF-2 activities of ER-α and the DNA-binding capacity of the AhR/Arnt heterodimer were dispensable (Supplementary Fig. 3a, lanes 4–6).

Finally, we tested whether AhR-ligand-dependent AhR–ER interaction was responsible for the oestrogenic actions of AhR agonists in the absence of oestrogens on gene expression in intact animals. In addition to the induction of the *CYP1A1* gene, treatments with 3MC (Fig. 4a) and TCDD (Fig. 4b) for 3 hours stimulated the expression of the oestrogen-responsive genes c-*fos*[25] and *vascular endothelial growth factor* (*VEGF*)[26] in the uteri of ovariectomized wild-type mice (Fig. 4a, b). This oestrogenic action of 3MC in the uterus was also detected in intact 21-day-old female mice, whereas the AhR agonists exhibited anti-oestrogenic activities in the presence of high doses of oestrogen (Fig. 4a). There have been conflicting reports on the induction of c-*fos* by AhR ligands: one is that AhR ligands repress the E2-induced expression of c-*fos*[3]; the other is that AhR ligands themselves induce the expression of c-*fos*[27]. The 3MC-mediated activation of oestrogen target genes was completely abolished in both $AhR^{-/-}$ (ref. 28) and ER-$\alpha^{-/-}$ (ref. 29) ovariectomized mice, although each receptor knockout mouse strain retained ligand responsiveness (Fig. 4a) and the expression (Supplementary Fig. 4a) of the other intact receptor. The injection of 3MC led to increases in uterine wet weight, as did that of E2 (Fig. 4c). This action of 3MC was again abolished in both $AhR^{-/-}$ and ER-$\alpha^{-/-}$ mice (Fig. 4c).

To examine whether the increased uterine wet weight was due to the proliferation of endometrial cells, DNA synthesis in uterine epithelial cells was examined by labelling with bromodeoxyuridine (BrdU). Ovariectomized mice treated with 3MC exhibited enhanced cell proliferation in the glandular epithelium, as did E2-treated mice (Fig. 4d). Proliferation of the luminal epithelium was enhanced by E2 but not by 3MC.

The present findings indicate that the oestrogenic action of AhR agonists might be exerted through a direct interaction between AhR/Arnt and unliganded ER and by the formation of functional units bound to EREs that activate transcription, at least in uterine gene induction and cellular proliferation. The most marked manifestation of the possible oestrogenicity of dioxins could be seen as their linking to endometriosis[4–7], because oestrogen is the major factor in the stimulation of proliferation of these cells. Thus, AhR expressed in the uterine glandular epithelium[30] might respond to dioxins by associating with unliganded ERs, which then stimulates oestrogen-dependent cell proliferation. In contrast, AhR agonists exhibit anti-oestrogenic activities in the presence of high doses of E2 in animals[3] and cultured cell lines[2]. We also found that AhR/Arnt repressed E2-bound ER function, which is consistent with these previous reports. However, whereas most previous studies have not examined or mentioned the effects of AhR ligands in the absence of E2, we addressed this issue carefully in the present study. Thus, oestrogen concentrations, which vary with age, oestrous cycle, tissues and other factors, might define the oestrogenic/anti-oestrogenic actions of the AhR ligands in intact animals. Our present model, in which AhR potentiates unliganded ERs but represses liganded ER, might be an explanation of these previous findings, and it will be of interest to identify the other components of the liganded AhR–ER-α complex involved in the oestrogenic/anti-oestrogenic actions of dioxins. Our proposal is that one of the molecular mechanisms for the oestrogen-related adverse effects of dioxin-type environmental contaminants is the modulation of oestrogen receptor signalling by dioxin-dependent association with dioxin receptor. □

Methods

Plasmids

Full-length complementary DNAs of AhR and Arnt were inserted into pcDNA3 vectors (Invitrogen). Three consensus EREs[16] and XREs[22] were inserted into the promoter of luciferase pGL3-basic vector to generate ERE-TATA–luciferase and XRE-TATA–luciferase, respectively. ER-α ΔAhR was generated by the deletion of 45–131 residues from ER-α. The other mutants of ER-α and ER-β were as described previously[21].

Transfection and luciferase assay

Human endometrium cancer-derived Ishikawa cells, human breast cancer-derived MCF-7 cells, green monkey COS-1 cells and human 293T cells maintained in DMEM supplemented with 10% FBS were cultured in phenol-red-free DMEM containing 0.2% charcoal-stripped FBS before assays. Cells at 40–50% confluence were transfected with the indicated plasmids (0.25 μg ERE-Luc, 0.1 μg XRE-Luc, 0.025 μg ER-α, AhR and Arnt were transfected) using Lipofectamine reagent (Gibco BRL) in 12-well Petri dishes. Total amounts of cDNA were adjusted by supplementing with empty vector up to 1.0 μg. Cells were treated with E2 (100 nM) and 3MC (1 μM). Luciferase activity was determined with the Luciferase Assay System (Promega)[16]. As a reference plasmid to normalize transfection efficiency, 25 ng pRL-CMV plasmid (Promega) was co-transfected in all experiments. Results are given as means ± s.d. for at least three independent experiments.

Immunoprecipitation and GST pull-down assay

Whole cell extracts[17] were used for immunoprecipitation with either anti-ER-α or anti-Flag antibody (anti-ER-α Ab-4 from Neo Markers; anti-Flag from Santa Cruz Biotechnology) after western blotting with anti-ER-α (Chemicon), anti-Arnt (Santa Cruz Biotechnology), anti-AhR (Santa Cruz Biotechnology), anti-p300 (Upstate Biotechnology), anti-SRC-1 (Santa Cruz Biotechnology), anti-Flag, anti-haemagglutinin and anti-Myc (Invitrogen) antibodies. Normal mouse immunoglobulin was used as a control. For immunoprecipitation of overexpressed proteins, cells were transfected as indicated with Flag-tagged ERs (5 μg), haemagglutinin-tagged AhR (3 μg), Myc-Arnt (5 μg), SRC-1 (0.7 μg) and p300 (0.7 μg) in the presence or absence of 3MC and E2. For the GST pull-down assay, AhR and Arnt were translated *in vitro* and incubated with either GST, GST–ER-α(A/B) or GST–ER-β(A/B) immobilized on glutathione–Sepharose beads[17].

Purification and separation of AhR-interacting complexes

HeLa nuclear extracts were loaded on an M2 anti-Flag agarose gel (Kodak). After being washed with binding buffer, the bound proteins were eluted from the agarose by incubation overnight with 2.5–5.0 ml of the Flag peptide (Kodak) in binding buffer (0.2 mg ml^{-1}). For fractionation on a glycerol gradient, eluents were layered on the top of a 13-ml linear 100–10% glycerol gradient and centrifuged for 16 h at 40,000 r.p.m. in an SW40 rotor (Beckman). Each fraction was western blotted with anti-AhR, anti-ER-α and anti-p300 antibodies. The protein standards used were β-globulin (M_r 158K) and thyroglobulin (667K)[17].

Chromatin immunoprecipitation

Soluble chromatins of MCF-7 cells prepared with the acetyl-histone H4 immunoprecipitation assay kit (Upstate Biotechnology) were immunoprecipitated with antibodies against the indicated proteins. Specific primer pairs were designated to amplify the promoter regions of the c-*fos* (5′-GAAGAGTGGAGAAGGG-3′ and 5′-GAAGCTGTGCTTACGG-3′), *pS2* (5′-AAAGAATTAGCTTAGGCC-3′ and 5′-ACCTTAATCCAGGTCC-3′) or *CYP1A1* (5′-CTTCGCCATCCATTCC-3′ and 5′-GGGACTCCTCTTCGAC-3′) genes from the extracted DNA. Optimal PCR conditions to allow semiquantitative measurement were used on 2% agarose/Tris-acetate-EDTA gels[17]. As a usual condition, cells were treated with ligands for 45 min. The inductions of the target genes were examined by northern blot analysis in MCF-7 cells treated with the ligands for 3 h.

ABCD precipitation

Avidin resin (Promega) was incubated with biotin-conjugated consensus ERE oligonucleotides, followed by incubation with cell lysates in lysis buffer (20 mM HEPES, 100 mM KCl, 0.5 mM EDTA, 0.1% Triton X-100 and 1 mM dithiothreitol) for 30 min. The subsequent ERE–protein complexes trapped on the resin were then eluted and western blotted[24].

Oestrogen responses in uterus

Nine-week-old female C57BL/6 mice with the indicated genotypes were ovariectomized. After 2 weeks the mice were treated with 3MC (4 mg kg^{-1}), TCDD (40 μg kg^{-1}), and/or E2 (20 μg kg^{-1}) in olive oil for 3 h. Total RNA was extracted from the uteri by Isogen (Wako Co.) and then subjected to northern blot analysis with cDNAs for the target genes for E2 (c-*fos*, *VEGF*) and for 3MC (*CYP1A1*), with *GAPDH* cDNA (encoding glyceraldehydes-3-

phosphate dehydrogenase) as an internal control[16]. For experiments with intact mice, 21-day-old female mice were used.

For uterine weight analysis, mice were treated with ligands for 3 days, and the ratio of uterine wet weight to body weight was calculated, followed by *t*-test analysis. Results are given as means ± s.e.m.

For the BrdU labelling experiment, ovariectomized mice were treated with ligands for 3 days, then injected with BrdU (30 mg kg^{-1}). Paraffin sections from the uteri 8 h after BrdU injection were immunostained with anti-BrdU monoclonal antibody by using the BrdU Labeling and Detection Kit 1 (Roche), and the percentage of BrdU-positive epithelial cells in the sections was calculated.

Received 19 February; accepted 1 April 2003; doi:10.1038/nature01606.

1. Bock, K. W. Aryl hydrocarbon or dioxin receptor: biologic and toxic responses. *Rev. Physiol. Biochem. Pharmacol.* **125**, 1–42 (1994).
2. Krishnan, V. *et al.* Molecular mechanism of inhibition of estrogen-induced cathepsin D gene expression by 2,3,7,8-tetrachlorodibenzo-*p*-dioxin (TCDD) in MCF-7 cells. *Mol. Cell. Biol.* **15**, 6710–6719 (1995).
3. Astroff, B. *et al.* Inhibition of the 17β-estradiol-induced and constitutive expression of the cellular protooncogene c-*fos* by 2,3,7,8-tetrachlorodibenzo-*p*-dioxin (TCDD) in the female rat uterus. *Toxicol. Lett.* **56**, 305–315 (1991).
4. Gibbons, A. Dioxin tied to endometriosis. *Science* **262**, 1373 (1993).
5. Mayani, A., Barel, S., Soback, S. & Almagor, M. Dioxin concentrations in women with endometriosis. *Hum. Reprod.* **12**, 373–375 (1997).
6. Rier, S. E., Martin, D. C., Bowman, R. E., Dmowski, W. P. & Becker, J. L. Endometriosis in rhesus monkeys (*Macaca mulatta*) following chronic exposure to 2,3,7,8-tetrachlorodibenzo-*p*-dioxin. *Fundam. Appl. Toxicol.* **21**, 433–441 (1993).
7. Cummings, A. M., Metcalf, J. L. & Birnbaum, L. Promotion of endometriosis by 2,3,7,8-tetrachlorodibenzo-*p*-dioxin in rats and mice: time–dose dependence and species comparison. *Toxicol. Appl. Pharmacol.* **138**, 131–139 (1996).
8. Brown, N. M., Manzolillo, P. A., Zhang, J. X., Wang, J. & Lamartiniere, C. A. Prenatal TCDD and predisposition to mammary cancer in the rat. *Carcinogenesis* **19**, 1623–1629 (1998).
9. Davis, B. J., McCurdy, E. A., Miller, B. D., Lucier, G. W. & Tritscher, A. M. Ovarian tumors in rats induced by chronic 2,3,7,8-tetrachlorodibenzo-*p*-dioxin treatment. *Cancer Res.* **60**, 5414–5419 (2000).
10. Sogawa, K. & Fujii-Kuriyama, Y. Ah receptor, a novel ligand-activated transcription factor. *J. Biochem. (Tokyo)* **122**, 1075–1079 (1997).
11. Schmidt, J. V. & Bradfield, C. A. Ah receptor signaling pathways. *Annu. Rev. Cell Dev. Biol.* **12**, 55–89 (1996).
12. Kato, S. *et al.* Activation of the estrogen receptor through phosphorylation by mitogen-activated protein kinase. *Science* **270**, 1491–1494 (1995).
13. McKenna, N. J. & O'Malley, B. W. Combinatorial control of gene expression by nuclear receptors and coregulators. *Cell* **108**, 465–474 (2002).
14. Mangelsdorf, D. J. *et al.* The nuclear receptor superfamily: the second decade. *Cell* **83**, 835–839 (1995).
15. Freedman, L. P. Increasing the complexity of coactivation in nuclear receptor signaling. *Cell* **97**, 5–8 (1999).
16. Watanabe, M. *et al.* A subfamily of RNA-binding DEAD-box proteins acts as an estrogen receptor alpha coactivator through the N-terminal activation domain (AF-1) with an RNA coactivator, SRA. *EMBO J.* **20**, 1341–1352 (2001).
17. Yanagisawa, J. *et al.* Nuclear receptor function requires a TFTC-type histone acetyl transferase complex. *Mol. Cell* **9**, 553–562 (2002).
18. Kamei, Y. *et al.* A CBP integrator complex mediates transcriptional activation and AP-1 inhibition by nuclear receptors. *Cell* **85**, 403–414 (1996).
19. Tian, Y., Ke, S., Thomas, T., Meeker, R. J. & Gallo, M. A. Transcriptional suppression of estrogen receptor gene expression by 2,3,7,8-tetrachlorodibenzo-*p*-dioxin (TCDD). *J. Steroid Biochem. Mol. Biol.* **67**, 17–24 (1998).
20. Tora, L. *et al.* The human estrogen receptor has two independent nonacidic transcriptional activation functions. *Cell* **59**, 477–487 (1989).
21. Kobayashi, Y. *et al.* p300 mediates functional synergism between AF-1 and AF-2 of estrogen receptor alpha and beta by interacting directly with the N-terminal A/B domains. *J. Biol. Chem.* **275**, 15645–15651 (2000).
22. Mimura, J., Ema, M., Sogawa, K. & Fujii-Kuriyama, Y. Identification of a novel mechanism of regulation of Ah (dioxin) receptor function. *Genes Dev.* **13**, 20–25 (1999).
23. Beischlag, T. V. *et al.* Recruitment of the NCoA/SRC-1/p160 family of transcriptional coactivators by the aryl hydrocarbon receptor/aryl hydrocarbon receptor nuclear translocator complex. *Mol. Cell. Biol.* **22**, 4319–4333 (2002).
24. Daitoku, H. Y. K., Matsuzaki, H., Hatta, M. & Fukamizu, A. Regulation of PGC-1 promoter activity by protein kinase B and the forkhead transcription factor FKHR. *Diabetes* **52**, 642–649 (2003).
25. Weisz, A. & Rosales, R. Identification of an estrogen response element upstream of the human c-*fos* gene that binds the estrogen receptor and the AP-1 transcription factor. *Nucleic Acids Res.* **18**, 5097–5106 (1990).
26. Mueller, M. D. *et al.* Regulation of vascular endothelial growth factor (VEGF) gene transcription by estrogen receptors alpha and beta. *Proc. Natl Acad. Sci. USA* **97**, 10972–10977 (2000).
27. Puga, A., Nebert, D. W. & Carrier, F. Dioxin induces expression of c-*fos* and c-*jun* proto-oncogenes and a large increase in transcription factor AP-1. *DNA Cell Biol.* **11**, 269–281 (1992).
28. Mimura, J. *et al.* Loss of teratogenic response to 2,3,7,8-tetrachlorodibenzo-*p*-dioxin (TCDD) in mice lacking the Ah (dioxin) receptor. *Genes Cells* **2**, 645–654 (1997).
29. Dupont, S. *et al.* Effect of single and compound knockouts of estrogen receptors α (ERα) and β (ERβ) on mouse reproductive phenotypes. *Development* **127**, 4277–4291 (2000).
30. Kuchenhoff, A. *et al.* Arylhydrocarbon receptor expression in the human endometrium. *Fertil. Steril.* **71**, 354–360 (1999).

Supplementary Information accompanies the paper on **www.nature.com/nature.**

Acknowledgements We thank K. Korach and A. Fukamizu for helpful discussion; T. Sato, A. Murayama and Y. Kobayashi for technical assistance; Taiho Pharmaceutical Co. for ER ligands; and R. Nakamura and H. Higuchi for manuscript preparation. This work was supported in part by grants-in-aid for priority areas from the Ministry of Education, Science, Sports and Culture of Japan (to Y.F.-K. and S.K.).

Competing interests statement The authors declare that they have no competing financial interests.

Correspondence and request s for materials should be addressed to S.K. (uskato@mail.ecc.u-tokyo.ac.jp).

Insulin-regulated hepatic gluconeogenesis through FOXO1–PGC-1α interaction

Pere Puigserver*†, James Rhee*, Jerry Donovan*, Christopher J. Walkey*, J. Cliff Yoon*, Francesco Oriente‡, Yukari Kitamura‡, Jennifer Altomonte§, Hengjiang Dong§, Domenico Accili‡ & Bruce M. Spiegelman*

* *Dana-Farber Cancer Institute and Department of Cell Biology, Harvard Medical School, Boston, Massachusetts 02115, USA*
‡ *Naomi Berrie Diabetes Center and Department of Medicine, College of Physicians & Surgeons of Columbia University, New York, New York 10032, USA*
§ *Institute for Human Gene Therapy and Molecular Medicine, Mount Sinai School of Medicine, New York, New York 10029, USA*

Hepatic gluconeogenesis is absolutely required for survival during prolonged fasting or starvation, but is inappropriately activated in diabetes mellitus. Glucocorticoids and glucagon have strong gluconeogenic actions on the liver. In contrast, insulin suppresses hepatic gluconeogenesis[1–3]. Two components known to have important physiological roles in this process are the forkhead transcription factor FOXO1 (also known as FKHR) and peroxisome proliferative activated receptor-γ co-activator 1 (PGC-1α; also known as PPARGC1), a transcriptional co-activator; whether and how these factors collaborate has not been clear. Using wild-type and mutant alleles of FOXO1, here we show that PGC-1α binds and co-activates FOXO1 in a manner inhibited by Akt-mediated phosphorylation. Furthermore, FOXO1 function is required for the robust activation of gluconeogenic gene expression in hepatic cells and in mouse liver by PGC-1α. Insulin suppresses gluconeogenesis stimulated by PGC-1α but co-expression of a mutant allele of FOXO1 insensitive to insulin completely reverses this suppression in hepatocytes or transgenic mice. We conclude that FOXO1 and PGC-1α interact in the execution of a programme of powerful, insulin-regulated gluconeogenesis.

Two transcriptional components that are targets of insulin signalling, and that can activate the process of gluconeogenesis in liver, are FOXO1 and PGC-1α. FOXO1 has been shown to bind directly to the promoters of gluconeogenic genes and activate the process of glucose production[4–6]. FOXO1 is directly phosphorylated by Akt, a key protein kinase downstream of the insulin receptor[7,8]. This phosphorylation results in exclusion of FOXO1 from the nucleus. A second transcriptional component controlled by insulin and having a role in gluconeogenesis is the co-activator PGC-1α. PGC-1α is induced in liver on fasting, and is elevated in several models of diabetes or deficiency in insulin signalling. Notably, expression of PGC-1α at physiological levels turns on the entire programme of gluconeogenesis[9,10].

† Present address: Department of Cell Biology, Johns Hopkins University School of Medicine, Baltimore, Maryland 21205, USA

Suppressive function of androgen receptor in bone resorption

Hirotaka Kawano*†‡, Takashi Sato*‡§, Takashi Yamada*†, Takahiro Matsumoto*§, Keisuke Sekine*, Tomoyuki Watanabe*, Takashi Nakamura*, Toru Fukuda*, Kimihiro Yoshimura*, Tatsuya Yoshizawa*, Ken-ichi Aihara*, Yoko Yamamoto*, Yuko Nakamichi*, Daniel Metzger¶, Pierre Chambon¶, Kozo Nakamura†, Hiroshi Kawaguchi†, and Shigeaki Kato*§‖

*Institute of Molecular and Cellular Biosciences and †Department of Orthopedic Surgery, Faculty of Medicine, University of Tokyo, 1-1-1 Yayoi, Bunkyo-ku, Tokyo 113-0032, Japan; §Solution-Oriented Research for Science and Technology, Japan Science and Technology Corporation, 4-1-8 Honcho, Kawaguchi, Saitama 332-0012, Japan; and ¶Institut de Génétique et de Biologie Moleculaire et Cellulaire, Centre National de la Recherche Scientifique, Institut National de la Santé et de la Recherche Médicale, Université Louis Pasteur, Collège de France, 67404 Illkirch, Strasbourg, France

Contributed by Pierre Chambon, June 6, 2003

As locally converted estrogen from testicular testosterone contributes to apparent androgen activity, the physiological significance of androgen receptor (AR) function in the beneficial effects of androgens on skeletal tissues has remained unclear. We show here that inactivation of AR in mice using a Cre-loxP system-mediated gene-targeting technique caused bone loss in males but not in females. Histomorphometric analyses of 8-week-old male AR knockout (ARKO) mice showed high bone turnover with increased bone resorption that resulted in reduced trabecular and cortical bone mass without affecting bone shape. Bone loss in orchidectomized male ARKO mice was only partially prevented by treatment with aromatizable testosterone. Analysis of primary osteoblasts and osteoclasts from ARKO mice revealed that AR function was required for the suppressive effects of androgens on osteoclastogenesis supporting activity of osteoblasts but not on osteoclasts. Furthermore, expression of the receptor activator of NF-κB ligand (*RANKL*) gene, which encodes a major osteoclastogenesis inducer, was found to be up-regulated in osteoblasts from AR-deficient mice. Our results indicate that AR function is indispensable for male-type bone formation and remodeling.

Steroid sex hormones are essential for normal skeletal development and maintenance of healthy bone remodeling during adult life (1, 2). Sex hormone status reflects bone mass, such that hormonal deficiency is well known to lead to progressive bone loss (3). The most striking example, osteoporosis in postmenopausal women, is a state of estrogen deficiency coupled with imbalanced bone remodeling, with higher bone resorption than bone formation, and can be rescued by estrogen replacement (4). Although androgens seem to exert beneficial effects in both males and females (3, 5), the physiological role of the androgen–androgen receptor (AR) system in skeletal tissues has not yet been well established. This is because estrogens are locally converted from serum androgens by aromatase present in bone and seem to contribute to the overt androgen effects on the skeleton (5, 6). This concept is supported by observations that male mice deficient in either aromatase or skeletal major estrogen receptor (ERα) suffer bone loss (6, 7). However, a number of studies have demonstrated that androgen treatment is protective against bone loss caused by the impaired estrogen signaling (3, 5), raising the possibility that AR-mediated androgen effects in bone remodeling are physiologically significant and independent of estrogen actions.

AR is a member of the nuclear steroid/thyroid hormone receptor gene superfamily and acts as a ligand-inducible transcription factor (8, 9). Most androgen effects are thought to be exerted through the transcriptional control of particular sets of target genes by AR. Upon hormone binding, AR is translocated from the cytosol into the nucleus and binds specific promoter elements. A number of coregulators and/or coregulator complexes are then recruited to AR, which then activates or represses the transcription of various target genes (10–13). Like the well described target tissues for androgens, bone tissues also express AR, being present in both osteoblasts and osteoclasts (2). Reflecting this AR expression, androgens have been shown to regulate the expression of several genes encoding growth factors and cytokines that control bone remodeling via both osteoblasts and osteoclasts (2). However, the role of AR in bone cell gene expression has not been well studied because of the lack of animals and cell lines deficient in AR expression.

To define the physiological functions of AR in target tissues, an AR-null mutant mouse line was generated by means of the Cre–loxP system, which was used to circumvent the problem of male infertility (14). The present study found that 8-week-old male AR knockout (ARKO; $AR^{L-/Y}$) mice developed osteopenia and exhibited retarded growth curves, although normal bone shape was retained and overt phenotypes were indistinguishable from those of WT female littermates. Although high bone turnover, with more bone resorption than formation, was seen in 8-week-old $AR^{L-/Y}$ male mice, female ARKO ($AR^{L-/L-}$) mice seemed normal with respect to bone mass and bone remodeling. These findings suggest that AR function was essential for male-type bone mass and bone remodeling. Furthermore, up-regulation of receptor activator of NF-κB ligand (*RANKL*) gene expression, along with enhanced potency to induce osteoclastogenesis in an *in vitro* coculture system, was observed for AR-deficient osteoblasts. Taken together, our results indicate that AR performs a suppressive function in osteoblasts during osteoclastogenesis that is indispensable for normal male-type bone formation and remodeling.

Materials and Methods

Animals. ARKO mice with the original C57BL6/CBA hybrid background were generated and maintained as reported (14). All mice were maintained according to the protocol approved by the Animal Care and Use Committee of the University of Tokyo.

Identification of AR Transcript by RT-PCR. Total mRNA was extracted from excised femora and tibiae by using an Isogen kit (Wako Pure Chemical, Osaka) and reverse transcribed by using XL reverse transcriptase (Takara Shuzo, Otsu, Japan) and an oligo(dT) primer (Takara Shuzo). After first-strand cDNA synthesis, 5% of the reaction mixture was amplified with r-*Taq*DNA polymerase (Takara Shuzo) by using specific primer pairs: 5′-CATGTAGGCCATGAGGTCCACCAC-3′ and 5′-TGAAGGTCGGTGTGAACGGATTTGGC-3′ for G3PDH;

Abbreviations: AR, androgen receptor; ARKO, AR knockout; ER, estrogen receptor; BMD, bone mineral density; DHT, 5α-dehydrotestosterone; RANKL, receptor activator of NF-κB ligand; TRAP, tartrate-resistant acid phosphatase; M-CSF, macrophage colony-stimulating factor.

‡H.K. and T.S. contributed equally to this work.

‖To whom correspondence should be addressed. E-mail: uskato@mail.ecc.u-tokyo.ac.jp.

www.pnas.org/cgi/doi/10.1073/pnas.1533500100

5′-TGGTAGCTGGTACTTCTAATGC-3′ and 5′-CATAAGGTCCGGAGTAGTTCTC-3′ for AR-1; and 5′-CAGAAGTATCTATGTGCCAG-3′ and 5′-ATCTTCTGGGATGGGTCCTCAG-3′ for AR-2. Up to 35 cycles of amplification were performed, with each cycle consisting of 96°C for 30 s, 55°C for 60 s, and 72°C for 60 s.

Analysis of Skeletal Morphology. Bone radiographs of excised femora and tibiae from 8-week-old WT and ARKO littermates were taken by using a soft x-ray apparatus (CMB-2; Softex, Tokyo). Three-dimensional computed tomography scanning was performed by using a composite x-ray analyzing system (NX-HCP; NS-ELEX, Tokyo). Bone mineral density (BMD) was measured by dual energy x-ray absorptiometry using a bone mineral analyzer (Piximus densitometer; Lunar, Madison, WI). Skeletal preparations for morphology were performed as described (15). Trabecular bone parameters were measured in an area 1.2 mm in length from 0.1 mm below the growth plate at the proximal metaphysis of tibiae, and cortex bone parameters were measured at the midshaft of femora.

Orchidectomy and Hormone Replacement. Male WT and ARKO littermates were orchidectomized or sham operated at 3 weeks of age and implanted s.c. with a slow-releasing pellet (10 mg/60 days) (Innovative Research of America) of placebo, testosterone (T), or 5α-dehydrotestosterone (DHT). BMD of femora was compared among eight experimental groups at 8 weeks of age.

Measurement of Serum Bone Metabolic Markers. Serum osteocalcin and urinary deoxypyridinoline were measured as bone formation and resorption markers in male WT and ARKO mice. Blood was sampled at time of death, and urine was collected for 24 h before death by using oil-sealed bottles in metabolic cages (Kurea, Tokyo). Concentration of deoxypyridinoline was corrected according to urinary creatinine concentration.

Statistical Analysis. Group means were compared by ANOVA, and the significance of differences were determined by post hoc testing with Bonferroni's method.

***Ex Vivo* Osteoblast Cultures.** Osteoblast cultures were performed as described (15). For the cell proliferation assay, primary osteoblasts were inoculated at a density of 2×10^3 cells per well in a 96-multiwell plate for 2 days, and cell number was counted with cell-counting kit solution (Wako Pure Chemical) according to the manufacturer's protocol. For the measurement of alkaline phosphatase activity, primary osteoblasts were inoculated at a density of 5×10^4 cells per 24 multiwells and cultured in αMEM containing 10% FBS and 50 μg/ml ascorbic acid. After 14 days of culture, alkaline phosphatase activity in the cell lysate was measured by using a Wako ALP kit (Wako Pure Chemical).

Osteoclastogenesis in Coculture of Bone Marrow Cells and Osteoblasts. To visualize osteoclasts, staining for tartrate-resistant acid phosphatase (TRAP) activity is widely used (15). TRAP-positive multinucleated osteoclasts were generated from hemopoietic cells by coculturing with osteoblasts. As a source of hemopoietic cells, bone marrow cells (5×10^5 cells per well) and osteoblasts (5×10^4 cells per well) were isolated and placed in 0.5 ml per 24 multiwells of αMEM/10% FBS for 8 days in the presence of 10 nM $1\alpha,25(OH)_2D_3$ (16). To determine osteoclast survival, osteoclasts were isolated and cultured as described (15). The number of TRAP-positive and trypan blue-negative multinucleated cells were counted at 0, 12, 18, 24, and 48 h. Bone resorption activity was measured as described (15).

Osteoclastogenesis in Bone Marrow Cell Culture. Bone marrow cells were inoculated at a density of 5×10^5 cells per 24 multiwells and cultured in 1.0 ml per 24 multiwells of αMEM/10% FBS with 100 ng/ml macrophage colony-stimulating factor (M-CSF) for the first 48 h, after which 100 ng/ml M-CSF and 100 ng/ml RANKL were added and incubated for an additional 96 h. TRAP-positive multinucleated osteoclasts were then counted.

RT-PCR Analysis of *RANKL* Gene Expression. Semiquantitative RT-PCR was carried out on primary cultured osteoblasts for a number of osteoblastic factor genes (17). After osteoblasts were cultured to confluency in αMEM containing 10% FBS, $1\alpha,25(OH)_2D_3$ (10 nM) was added with DHT (10 nM) or vehicle and cultured for 48 h. Total RNA extraction and reverse transcription was performed as described above. After first-strand cDNA synthesis, 5% of the reaction mixture was amplified with r-*Taq*DNA polymerase (Takara Shuzo) by using specific primer pairs 5′-GCATCGCTCTGTTCCTGTA-3′ and 5′-GTGCTCCCTCCTTTCATCA-3′ for RANKL and G3PDH. Up to 25 cycles of amplification were performed, with each cycle consisting of 96°C for 30 s, 55°C for 60 s, and 72°C for 60 s.

Results

Male ARKO Mice Exhibit Abnormalities Typical of Testicular Feminization Mutant Rodents. To avoid male infertility caused by AR mutation, thereby preventing the establishment of a line of AR-deficient mice, we applied the Cre-loxP system to first flox the *AR* gene on the sole X chromosome in male mice (14). Floxed male mice ($AR^{L3/Y}$) (Fig. 1*a*) seemed completely normal with regard to bone mass and reproduction and showed no apparent differences from WT littermates. Male ARKO ($AR^{L-/Y}$) mice, descended from female AR heterozygotes ($AR^{+/L-}$), showed growth retardation compared with male littermates, but growth curves and external reproductive organs were indistinguishable from those of female littermates up to 8 weeks of age (Fig. 1*b*). Reflecting the atrophic testis in 8-week-old $AR^{L-/Y}$ mice, testicular androgen production seemed to be severely impaired, leading to marked reduction in serum gonadal androgen levels, whereas serum estrogen and adrenal androgen levels remained unchanged (Fig. 1*c*). Thus, the phenotypic abnormality of $AR^{L-/Y}$ mice seemed identical to that reported for testicular feminization mutant rodents, natural mutants with AR dysfunction (3, 10). To our surprise, female ARKO ($AR^{L-/L-}$), which never exist in nature, exhibited no phenotypic abnormality up to 8 weeks of age. However, it was possible that the abnormal AR protein derived from the genetically mutated AR gene locus still retained some level of androgen responsiveness (18). To address this issue, the presence of AR transcripts in bone in both male ($AR^{L-/Y}$) and female ($AR^{L-/L-}$) ARKO mice was assessed. No transcripts were detected by Northern blotting (data not shown) or by RT-PCR using several primer pairs performed on total bone tissue (Fig. 1*d*). These findings established that our ARKO mouse was indeed a mammalian AR-null mutant model.

Osteopenia in Male ARKO Mice. To examine the physiological roles of AR in mediating androgenic effects on bone tissue, we first analyzed the skeletal morphology of $AR^{L-/Y}$ mice. Soft x-ray analysis revealed severe osteopenia of femora and tibiae from 8-week-old male mice (Fig. 1*e*), but also that bone shape and bone length (Figs. 1*e* and 2*b*) were not affected by AR inactivation. This was consistent with the clear loss in radiographic BMD of femora from $AR^{L-/Y}$ mice compared with WT male littermates. The BMD of $AR^{L-/Y}$ mice was even lower than that of WT female littermates (Fig. 2*a*). Three-dimensional computed tomography scan analysis of femora showed that bone loss in $AR^{L-/Y}$ mice occurred throughout the entire femur (Fig. 2*c*). Histomorphometric analysis of proximal tibiae from $AR^{L-/Y}$ mice confirmed that trabecular bone volumes (bone volume per tissue volume: BV/TV) were markedly decreased, whereas no overt differences in growth plates were detected between

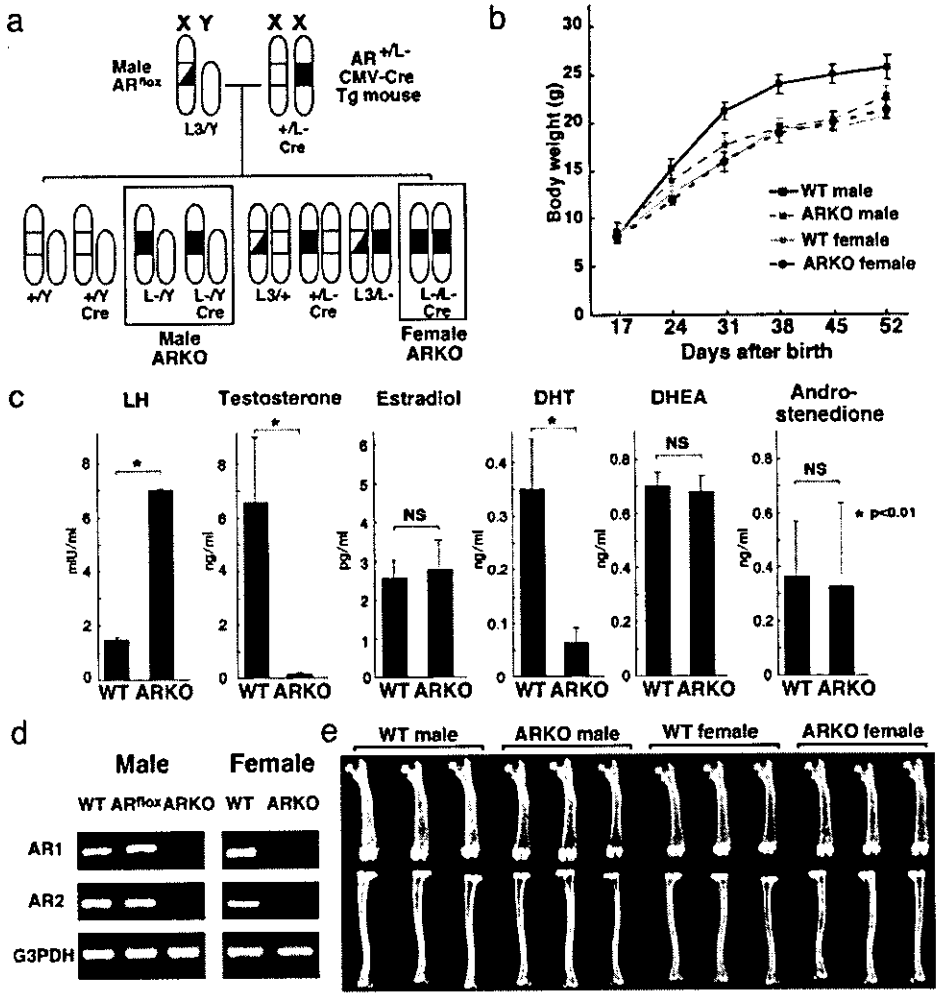

Fig. 1. (*a*) Strategy to generate male and female ARKO mice using CMV-Cre transgenic mice. (*b*) Growth curves of ARKO and WT littermate mice. (*c*) Serum hormone levels in 8-week-old ARKO and WT mice. (*d*) Lack of AR expression in bone of ARKO mice (RT-PCR). (*e*) Soft x-ray images of femora and tibiae from 8-week-old ARKO and WT mice.

$AR^{L-/Y}$ and WT mice (Fig. 2*d*). Such bone loss was also evident in cortical bones as estimated by cortex thickness (Fig. 2*e*). In contrast, no clear loss of bone mass was detected in female ARKO mice (Figs. 1*e* and 2*a*). Together, these findings suggest that $AR^{L-/Y}$ mice developed osteopenia, which implies that the AR function is required for male-type bone mass and remodeling.

The Suppressive Function of AR in Bone Resorption Is Abrogated in Male ARKO Mice. To further study the process of bone loss in $AR^{L-/Y}$ mice, bone remodeling was assessed. The bone formation rate of the trabecular bone was directly estimated by calcein double-labeling of the mineralized matrix (17). Unexpectedly, the bone formation parameters (Ob.S/BS and MAR) were significantly increased in $AR^{L-/Y}$ mice, with increased thickness of the region between the two calcein-labeled layers compared with WT littermates (Fig. 3*a*). This increased bone formation was also found in the cortical bone, in the endocortical area of the axial section (Fig. 3*b*). We observed an increase in the number of TRAP-positive mature osteoclasts (Fig. 3*c*). This was reflected in the significantly increased bone resorption parameters (Oc.S/BS, N.Oc/B.Pm) (Fig. 3*c*). Our finding of enhanced bone turnover was further supported by the increased levels of serum osteocalcin and urinary deoxypyridinoline (Fig. 3*d*). Although female ARKO mice exhibited no abnormal bone remodeling, our findings suggested that AR inactivation caused high turnover bone remodeling with higher bone resorption than formation, resulting in the development of osteopenia in males.

Effects of Androgens Other Than Those from Locally Converted Estrogen on Male Bone Remodeling. It is thought that estrogen converted from serum testosterone by aromatase expressed in androgen target tissues, including bone, contributes to apparent androgen activity (6). As serum testosterone levels were drastically decreased due to atrophic testes in $AR^{L-/Y}$ mice, it was impossible to exclude the possibility that the osteopenia in $AR^{L-/Y}$ mice simply reflected the impaired action of converted estrogen from serum testosterone on skeletal tissues. To address this issue, aromatizable testosterone (T) and nonaromatizable androgen DHT were given to orchidectomized $AR^{L-/Y}$ and WT littermates, and the femur BMD was assessed. Whereas orchidectomy caused no further BMD loss in $AR^{L-/Y}$ femora, BMD values from orchidectomized WT littermates were higher, but not significantly, than those of $AR^{L-/Y}$ mice (Fig. 3*e*). Also, whereas T, but not DHT, effectively recovered BMD, the recovery in $AR^{L-/Y}$ mice due to T was only ≈50% of that in intact males (Fig. 3*e*), which suggests that androgen actions mediated via AR are significant in protecting against bone loss.

Suppressive Effects of AR on *in Vitro* Osteoclastogenesis and *RANKL* Gene Expression in Osteoblasts. To further explore the mechanisms of increased bone resorption in $AR^{L-/Y}$ mice, *in vitro* osteoclas-

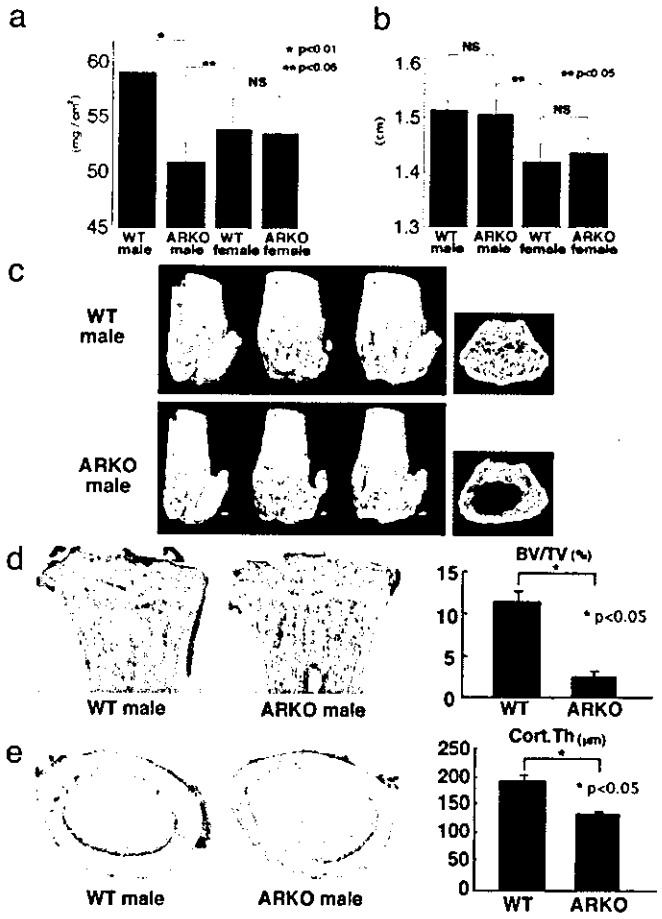

Fig. 2. Osteopenia in male ARKO mice. (*a*) Bone loss in femur of 8-week-old male ARKO mice by BMD analysis. (*b*) Bone length in 8-week-old ARKO and WT littermate mice. (*c*) Three-dimensional computed tomography images of distal femora and axial sections of distal metaphyses from representative 8-week-old male WT and ARKO littermates. (*d*) Histological features and histomorphometry of the proximal tibiae from 8-week-old male ARKO and WT mice. For Villanueva–Goldner staining of sections from representative ARKO and WT male littermates, mineralized bone is stained green. BV/TV, trabecular bone volume expressed as a percentage of total tissue volume. (*e*) Histological features and histomorphometry of the midshaft of femora of 8-week-old mice. Cort.Th., cortex thickness.

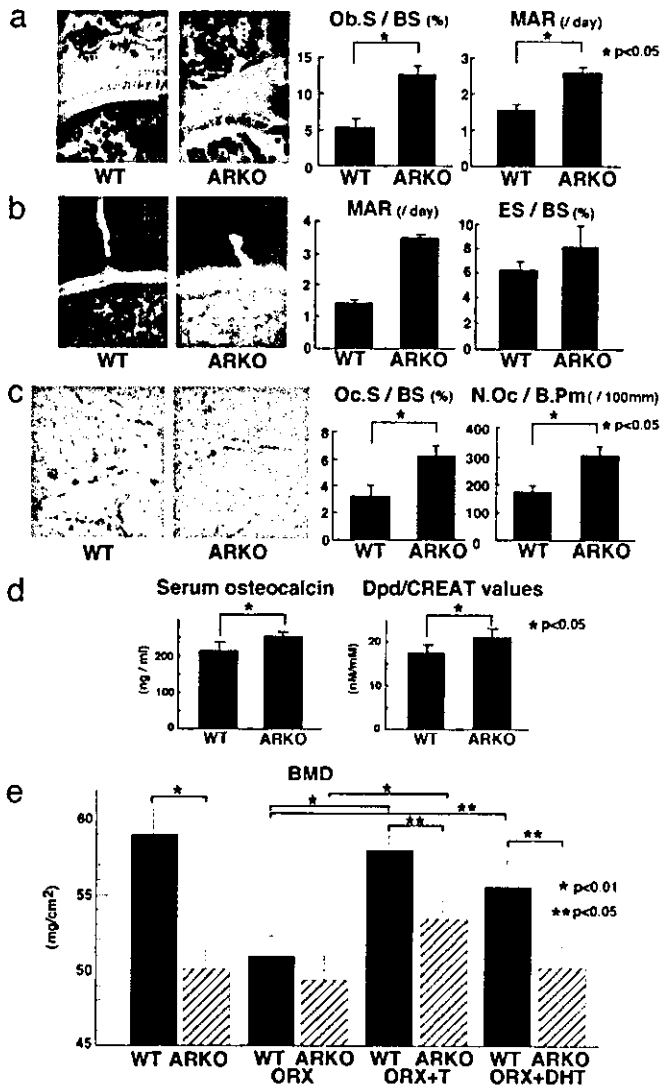

Fig. 3. High bone turnover in male ARKO mice and its partial prevention by an aromatizable androgen. (*a*) Two calcein-labeled mineralized fronts visualized by fluorescent micrography and bone formation parameters in the proximal tibia of 8-week-old male ARKO and WT littermate mice. Ob.S/BS, percentage of bone surface covered by cuboidal osteoblasts; MAR, mineral apposition rate. (*b*) Two calcein-labeled mineralized fronts and bone histomorphometric parameters in the midshaft of femora from 8-week-old male ARKO and WT littermate mice. ES/BS, percentage of eroded surface. (*c*) TRAP staining and bone resorption parameters in the proximal tibiae of 8-week-old male WT and ARKO mice. TRAP-positive osteoclasts on secondary spongiosa are stained red. Oc.S/BS, percentage of bone surface covered by mature osteoclasts; N.Oc/B.Pm, number of mature osteoclasts in 10 cm of bone perimeter. (*d*) Serum osteocalcin levels and urinary deoxypyridinoline levels of 8-week-old male ARKO and WT mice. (*e*) BMD values of femora from 8-week-old mice after orchidectomy (ORX) and hormone replacement. T, testosterone.

togenesis was assessed using osteoclast precursor cells from bone marrow and calvaria osteoblasts (16, 17) derived from male WT and $AR^{L-/Y}$ mice (Fig. 4*a*). TRAP-positive multinucleated osteoclasts were clearly cytodifferentiated by $1\alpha,25(OH)_2D_3$ stimulation even when AR was absent in osteoclast precursor cells (Fig. 4*a*). *RANKL* is a member of tumor necrosis factor-α superfamily cytokines, which induces osteoclastogenesis and activates osteoclast function. Consistent with normal osteoclastogenesis in response to $1\alpha,25(OH)_2D_3$, RANKL signaling activated by RANKL and M-CSF during osteoclastogenesis also seemed unaffected in AR-deficient osteoclasts (Fig. 4*c*). Moreover, resorption pits produced by cultured AR-deficient primary osteoclasts seemed normal both in terms of numbers and area when compared with osteoclasts from WT littermates (Fig. 4*b*). Surprisingly, the survival rate of osteoclasts in the presence of DHT was unaffected by AR inactivation (Fig. 4*d*), in sharp contrast to a recent report concerning the osteoclast survival function of AR (19). However, AR inactivation in osteoblasts seemed to potentiate osteoblastic functions that promote osteoclastogenesis in the presence of inducers (Fig. 4 *a* and *b*). However, we detected no abnormalities in cultured AR-deficient primary osteoblast cell proliferation by MTT [3-(4,5-dimethylthiazol-2-yl)-2,5-diphenyl tetrazolium bromide] assay or maturation by alkaline phosphatase activity (data not shown). In searching for the osteoblastic factor responsible for the increased osteoclastogenesis (20, 21), *RANKL* turned out to be transcriptionally up-regulated in AR-deficient osteoblasts (Fig. 4*e*). Thus, our findings suggest that the suppressive function of AR on *RANKL* gene expression mediates the protective effects of androgen on bone remodeling through the inhibition of bone resorption.

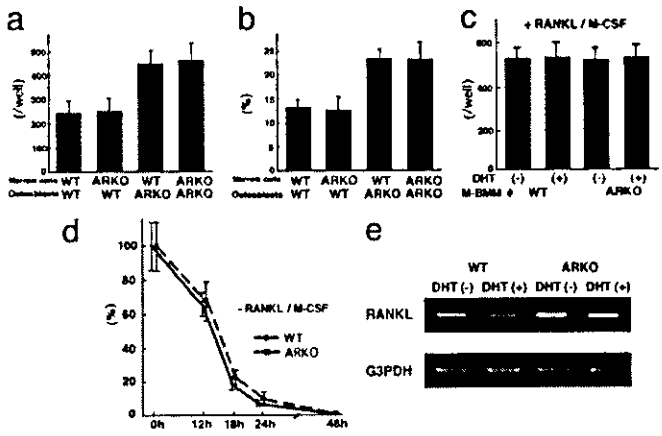

Fig. 4. (*a*) Osteoclastogenesis in bone marrow cell and osteoblast cocultures. TRAP-positive multinucleated osteoclast numbers were counted after 8-day coculture of bone marrow cells and osteoblasts from male ARKO and WT mice in the presence of 10 nM $1\alpha,25(OH)_2D_3$. (*b*) Pit area resorbed by osteoclasts over an additional 48-h period of coculture on a dentine slice. (*c*) Osteoclast formation in cultured M-CSF-dependent bone marrow macrophages. (*d*) Survival rate of isolated osteoclasts formed during coculture of osteoblasts and bone marrow cells. (*e*) Gene expression of *RANKL* and *G3PDH* in cultured primary osteoblasts from male ARKO and WT littermates.

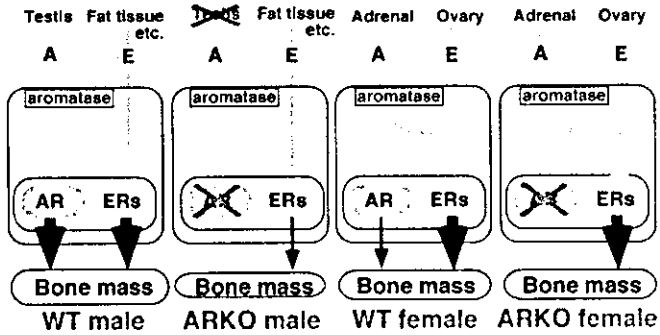

Fig. 5. Schema of skeletal sex hormone action. In male WT mice, skeletal sex hormone activities are mediated by both AR and ER. In female WT mice, skeletal function of ER is likely to dominate over that of AR as serum levels of AR ligands in females are quite low. In male ARKO mice, testicular testosterone production is severely impaired by hypoplasia of the testes, leading to a lack of skeletal sex hormone actions. In contrast, female ARKO mice may not be greatly affected by disruption of AR signaling.

Discussion

The present study, using orchidectomized ARKO mice, directly demonstrates that AR function is essential for androgen effects on the male skeleton. Although a number of previous studies have assessed the bone phenotypes of testicular feminization mutant rodents and humans eventually treated with sex hormones (3, 5), it has still been difficult to isolate AR functions in the skeletal system due to the local conversion of androgens to estrogens (6). When aromatizable testosterone (Fig. 3*e*) was given to orchidectomized ARKO mice, bone loss was only partially prevented, clearly establishing the pivotal function of AR in male-type bone remodeling. This finding is supported by previous reports concerning the beneficial effects of testosterone in male $ER\alpha^{-/-}$ and $ER\alpha\beta^{-/-}$ bone (22). As no clear bone loss in female ARKO mice was detected, AR is likely to be one of the determining factors in the formation of male-type bone, along with other AR downstream factors that may be encoded in male-specific Y chromosome regions. However, as bone loss was also induced by inactivation of either ERα or aromatase in male mice (23, 24), ER-mediated estrogen signaling also seems to be physiologically significant in the retention of male-type bone mass and bone remodeling. In such mice, high bone turnover with increased bone resorption was also observed. Therefore, it is possible that receptor-mediated signaling by both androgens and estrogens is convergent in the suppressive action on male bone resorption.

Unlike male ARKO mice, no overt differences in bone phenotype and mass were found between female AR-deficient and WT littermate mice at 8 weeks of age. Although the effects of anabolic androgens on bone have been documented in female rodents and humans, the physiological function of AR may not be significant because of the probably dominant role of ER function in female bones (Fig. 5), reflecting the high levels of serum estrogens in females. However, under certain conditions, such as estrogen deficiency in postmenopausal women (4), AR-mediated androgen effects may become physiologically significant in the protection against bone loss. This hypothesis will be tested using ovariectomized female ARKO mice in future studies.

The higher rate of bone resorption than formation with increased osteoclastogenesis observed in the $AR^{L-/Y}$ mice has been implied in previous reports (3, 5, 25). However, several recent reports (19, 26, 27) were inconsistent with our findings that osteoclast precursor cells were unaffected by AR deficiency in terms of cell survival and responsiveness to well characterized osteoclastogenesis inducers such as $1\alpha,25(OH)_2D_3$ and M-CSF (Fig. 4 *a–d*). Similar to AR, critical ERα functions in osteoclast precursor cells from ERα-deficient ($ER\alpha^{-/-}$) mice were not detected during *in vitro* osteoclastogenesis, and increased expression of the *RANKL* gene in osteoblast was also found (unpublished results). Together with previous findings of suppressive ERα effects on RANKL signaling (28), we speculate that the convergent functions of AR and ERα in male bone formation and remodeling are mediated through their suppressive functions on RANKL gene expression in osteoblasts. To test this hypothesis, identification of the negatively regulatory elements by receptors in the *RANKL* gene promoter (29) is clearly required.

We thank Dr. Yoshiaki Azuma and the hard tissue research team at Kureha Chemical for technical assistance and Dr. Toru Akune for helpful discussion. This work was supported in part by grants-in-aid from the Ministry of Education, Science, Sports and Culture of Japan (to S.K. for priority areas and to H. Kawano).

1. Bland, R. (2000) *Clin. Sci.* **98,** 217–240.
2. Compston, J. E. (2001) *Physiol. Rev.* **81,** 419–447.
3. Bilezikian, J. P. (2002) *J. Bone Miner. Res.* **17,** 563–566.
4. Riggs, B. L., Khosla, S. & Melton, L. J., III (2002) *Endocr. Rev.* **23,** 279–302.
5. Hofbauer, L. C. & Khosla, S. (1999) *Eur. J. Endocrinol.* **140,** 271–286.
6. Simpson, E. R. & Davis, S. R. (2000) *Proc. Natl. Acad. Sci. USA* **97,** 14038–14040.
7. Couse, J. F. & Korach, K. S. (1999) *Endocr. Rev.* **20,** 358–417.
8. Takeyama, K., Ito, S., Yamamoto, A., Tanimoto, H., Furutani, T., Kanuka, H., Miura, M., Tabata, T. & Kato, S. (2002) *Neuron* **35,** 855–864.
9. Mangelsdorf, D. J., Thummel, C., Beato, M., Herrlich, P., Schutz, G., Umesono, K., Blumberg, B., Kastner, P., Mark, M., Chambon, P., *et al.* (1995) *Cell* **83,** 835–839.
10. Wilson, J. D. (1999) *Endocr. Rev.* **20,** 726–737.
11. McKenna, N. J. & O'Malley, B. W. (2002) *Cell* **108,** 465–474.
12. Glass, C. K. & Rosenfeld, M. G. (2000) *Genes Dev.* **14,** 121–141.
13. Yanagisawa, J., Kitagawa, H., Yanagida, M., Wada, O., Ogawa, S., Nakagomi, M., Oishi, H., Yamamoto, Y., Nagasawa, H., McMahon, S. B., *et al.* (2002) *Mol. Cell* **9,** 553–562.
14. Sato, T., Matsumoto, T., Yamada, T., Watanabe, T., Kawano, H. & Kato, S. (2003) *Biochem. Biophys. Res. Commun.* **300,** 167–171.